Paleoecology and preservation of faunal assemblages in phosphatic nodules from the Pennsylvanian Midcontinent

Wells Thorne
Advisor: Derek Briggs
2nd Reader: Celli Hull
4/30/14

A Senior Thesis presented to the faculty of the Department of Geology and Geophysics, Yale University, in partial fulfillment of the Bachelor's Degree.

Abstract

The black "core" shales of the Pennsylvanian Midcontinent are most commonly thought to have been deposited in a deep-water marine environment under anoxic conditions, although historically the depositional environment of these shales has been a point of contention. Phosphatic nodules from these shales contain fossils that are exceptionally preserved in three-dimensions. These fossils can provide important insights into the paleoecology of the environment in which the nodules were formed. A sample of nodules collected from the Missourian Tacket Shale of Tulsa, Oklahoma were split and their contents identified and sorted into broad taxonomic groups. Certain nodules were selected for additional examination via scanning electron microscopy and elemental analysis using energy-dispersive X-ray spectroscopy. The nodules contained fossils representing a faunal community that consisted primarily of bony and cartilaginous fishes, cephalopods (ammonoids, nautiloids, and coleoids), orbiculoid brachiopods and unidentified arthropods. This largely nektonic assemblage is consistent with the interpretation that the shales were deposited under anoxic conditions that could not support diverse benthic communities.

The fossil remains are preserved largely in apatite. In some instances, phosphate replacement was followed by secondary encrustation in apatite crystals. Regardless of whether they are encrusted, none of the specimens examined under SEM display original microstructure. Phosphatic encrustation produces a distinctive botryoidal texture, created by clusters of elongated, radially oriented crystals. Similar textures of phosphate crystals have been controversially interpreted as fossilized microbes.

Examination of the Tacket Shale nodules provided no evidence supporting this hypothesis. However, encrusted tubular microstructures were also found in several nodules; these are much more likely to represent microbial remains.

Introduction

Phosphatic nodules are commonly found within the black and dark gray shales of the Midcontinent Pennsylvanian outcrop belt. These shales form part of a cyclic sequence of alternating shales and limestones representing eustatic fluctuations in the epicontinental sea (Heckel 1986, 1991). This sequence, called the "Kansas cyclothem", begins with a sandy, nearshore shale indicating minimum sea level (Heckel 1986, 1991; Kidder et al. 1996). It is followed first by a transgressive limestone, and then by an offshore, black or gray "core" shale that represents maximum transgression (Heckel 1986, 1991; Kidder et al. 1996). Lastly, a regressive limestone is deposited on top of the core shale; the cycle then continues with another nearshore shale (Heckel 1986, 1991; Kidder et al. 1996).

Figure 1: A generalized Kansas cyclothem of the Midcontinent Pennsylvanian (from Heckel 1986, p. 330).

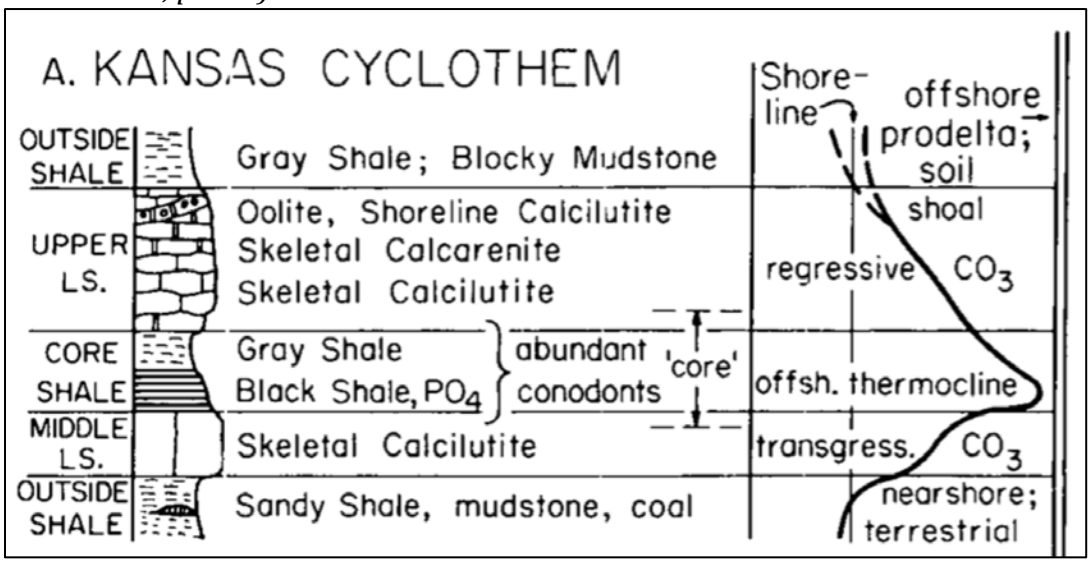

The depositional environment of the organic-rich, phosphatic "core" shales has been the subject of intensive study. Zangerl and Richardson (1963) considered the organic-rich shales to be shallow-water deposits laid down under brackish conditions. Heckel (1977) contested this model, suggesting instead that the core shales were deposited in a relatively deep open-marine environment. This deep-water interpretation was reinforced by subsequent paleontological and petrological evidence from studies by Boardman et al. (1984) and Kidder (1985). Schram (1984) noted that the presence in these shales of distinctively marine crustaceans, such as tyrannophontid stomatopods, was incompatible with the brackish-water hypothesis of Zangerl and Richardson (1963). Heckel (1991, p. 262) summarized the evidence supporting a deep-water, open-marine depositional environment:

"The combination of [the core shale's] position between the two marine limestone members, its thinness but broad lateral extent, the presence of non-skeletal phosphorite, the abundance of conodonts, the high organic carbon content, and the lack of coarse terrigenous debris, establishes the deposition of the core shale under conditions of near sediment starvation and bottom-water dysoxia (gray facies) to anoxia (black facies), far from shore during the highest stands of sea level."

Coveney et al. (1991) proposed two subgroups of black phosphatic shale, arguing that, while one type was formed under the deep-water conditions proposed by Heckel (1977), the other was deposited in shallow water. The debate regarding the validity of this subdivision is ongoing (Heckel and Hatch 1992; Coveney et al. 1992).

Those core shales that are generally recognized as deep-water deposits contain black and dark gray facies, the latter having been deposited in slightly shallower, more oxygenated water than the black shale (Heckel 1991). The black facies is either overlies or is sandwiched within the gray facies (Heckel 1991). Heckel described how a transgression maximum could lead to the deposition of black shale, explaining that "long-term density stratification" is most likely to develop when sea level is highest (Heckel 1991, p. 263). This type of stratification, known as a pycnocline, prevents vertical circulation of oxygen, thus leading to "greater preservation of organic matter in the sediment, establishment of an anoxic bottom environment, and ultimately to the formation of black shale" (Heckel 1991, p. 263).

Although nodules can be found throughout the black shale facies, they are often concentrated near the contact between the gray and black facies (Kidder 1985; Kidder et al. 1996). There is also evidence that the nodules are largest at the contact (Kidder 1985; Kidder et al. 1996). Heckel (1991) proposed that upwelling of phosphate-rich, oxygen-poor water from the sea bottom created the chemical conditions required for nodule formation. He noted that the contact between the black shale and the overlying gray shale, where nodules are the largest and most abundant, represents "the stratigraphic position corresponding to sufficient

shallowing that the stable stratification was being destroyed" (Heckel 1991, p. 267). As the pycnocline broke down and bottom conditions began to shift from anoxic to dysoxic, "any upwelling of deeper anoxic phosphate-rich water would have entered the shallower, more oxygenated and slightly warmer layer where phosphate would have been most readily precipitated" (Heckel 1991, p. 267).

Buried fecal matter is sometimes assumed to be the primary source of the high phosphate concentrations in the bottom water (Kidder and Eddy-Dilek 1994; Dalton et al. 1998). Kidder (1985) explored the mechanism of phosphate enrichment in more detail. Revisiting a model originally proposed by Heckel (1977), Kidder proposed that the upwelling conditions would have created "a circulatory nutrient trap…rich in planktonic life" (Kidder 1985, p. 814). Thus, the seabed would be constantly supplied with phosphorus not only from fecal matter but also from the phosphorus-rich bodies of dead plankton. The release of phosphorus into the sediment would create an environment allowing apatite to precipitate onto substrates that would ultimately become the nuclei of concretions (Kidder 1985, p. 814-815; Dalton et al. 1998). A significant amount of the dissolved phosphate could also come from decaying fish debris (Suess 1981).

The nodules are frequently assumed to be coprolitic (Kidder et al. 1996; Dalton et al. 1998; Kidder et al. 2003; Murthy et al. 2004). Indeed, very well-preserved coprolites have been recovered from phosphate nodules in Carboniferous black shales (Fugitt et al. 1994; Krishnaswamy et al. 1994). Specifically, the nodules reported by Fugitt et al. (1994) and Krishnaswamy et al. (1994) preserve spiral structures that are

easily identifiable as shark feces. The contents of a shark's spiral-shaped intestinal valve can fossilize to produce an endocast, or cololite, that replicates minute details of the shark's intestinal tract (Williams 1972). The characteristic spiral shape of the cololite makes it one of the easiest kinds of fossilized feces to recognize (Chin 2002). Given that many of the phosphatic nodules that other authors have assumed to be coprolitic lack such obvious defining traits, the question remains as to whether the classification of all such nodules as coprolites is valid.

Formation of the nodules seems to have occurred early in diagenesis. The host shales are deformed around the concretions, and the concretions themselves have nuclei that are preserved in three dimensions, suggesting that the concretions lithified prior to compaction of the surrounding mud (Zangerl et al. 1969, p. 118; Kidder 1985, p. 809; Molineux et al. 1995). Moreover, the concretions demonstrate excellent preservation of soft parts that would have decayed had fossilization not occurred fairly quickly (Heckel 1991, p. 269; Murthy et al. 2004, p. 100). Most studies of the paleoenvironment in which the nodules formed have focused on stratigraphy and sedimentology. Paleoecological analyses of the diversity of remains within the nodules can contribute valuable information to supplement this stratigraphic evidence and ultimately provide a clearer picture of the conditions represented by the black shale facies (e.g. Malinky and Heckel 1998).

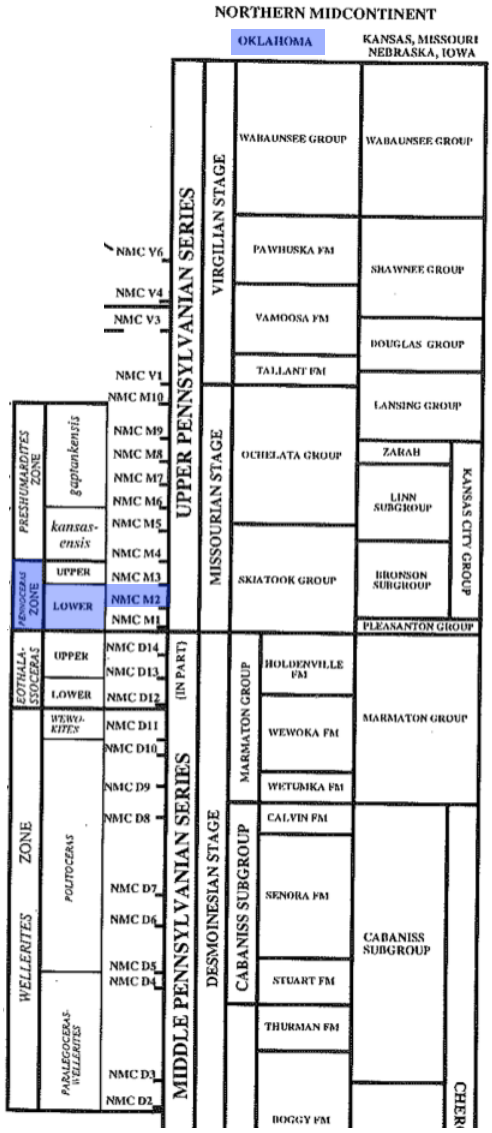

Figure 2: The stratigraphy of the Northern American midcontinent. Note the Pennoceras *zone and the NMC M2 horizon of the lower Tacket Shale, highlighted in blue. Modified from Boardman et al. (1994, p. 39).*

Methods

A total of 1,876 phosphatic nodules from the Tacket Shale (Missourian, Upper Pennsylvanian) of Tulsa, Oklahoma were examined (Figure 2). The nodules were collected in July 2012 at the locality designated by Boardman et al. (1994) as OKM-40 (Coffeyville Formation, Horizon NMC M2, *Pennoceras* Zone). Boardman et al.

(1994, p. 86) provide the following locality information: “Center south line of NW sec. 26, T. 19 N., R. 12 E., Sapulpa North 7 ½’ Quadrangle, Tulsa County, Oklahoma; hillside exposure”. In the classification system of the American Museum of Natural History, this locality is known as AMNH 3515. The nodules, which had eroded out of the surrounding shale, were collected indiscriminately from the surface using shovels (Kruta, personal comm., 2013). Before any nodules were broken, they were rinsed so that any fossil material on the exterior of the nodule would be visible. Some nodules had broken open prior to their collection or in transit, and their contents could be observed. Eighteen nodules with shapes suggesting they contained paleoniscid or chondrichthyan braincases were left unbroken at the request of the vertebrate paleontology department at AMNH. Intact braincases are valuable as they can be examined via CT scan and used for 3D reconstruction of the brain (e.g. Pradel et al. 2009). The remaining nodules were broken, parallel to bedding, with a rock splitter.

Nodules containing material that was not identifiable to the naked eye were further examined using a light microscope. Once all the nodules had been split and the fossils identified to the best of my ability, the number of each broad category of fossil was recorded, as was the number of barren nodules. Specific fossils were selected for examination via scanning electron microscopy. These included eleven nodules containing crushed material, which were selected for the purpose of determining whether the macerated contents could be identified by the details of the microstructure. Certain nodules were also subjected to elemental analysis using energy-dispersive X-ray spectroscopy.

Results

Table 1: Contents of split nodules

Contents	Taxon		Count
Fossiliferous	Paleoniscid	Bone	54
		Braincase	12
		Scale	25
	Chondrichthyan	Cartilage	44
		Listracanthus spines	54
	Vertebrate (unidentified)		22
	Ammonoid	Shell	12
		Radula + shell debris	1
	Nautiloid	Shell	2
	Coleoid	Arm hooks	2
	Cephalopod (unidentified)	Shell	6
		Jaw	1
	Mollusk (unidentified)	Shell	8
	Brachiopod		12
	Arthropod		4
	Plant material		1
	Coprolite (?)		3
	Unidentified		371
		Subtotal	**634**
Dubious - contents cannot be determined to be fossiliferous			738
Empty - no fossil content			486
Total			**1858**

The nodules contain both vertebrate and invertebrate remains, as well as one instance of fossilized plant material (Table 1). The bony fishes present in this fossil assemblage belong to the Palaeonisciformes, a group of stem actinopterygians. They are represented by pieces of bone, scales of various shapes and, most notably, braincases, which are exceptionally preserved in three dimensions (Fig. 3).

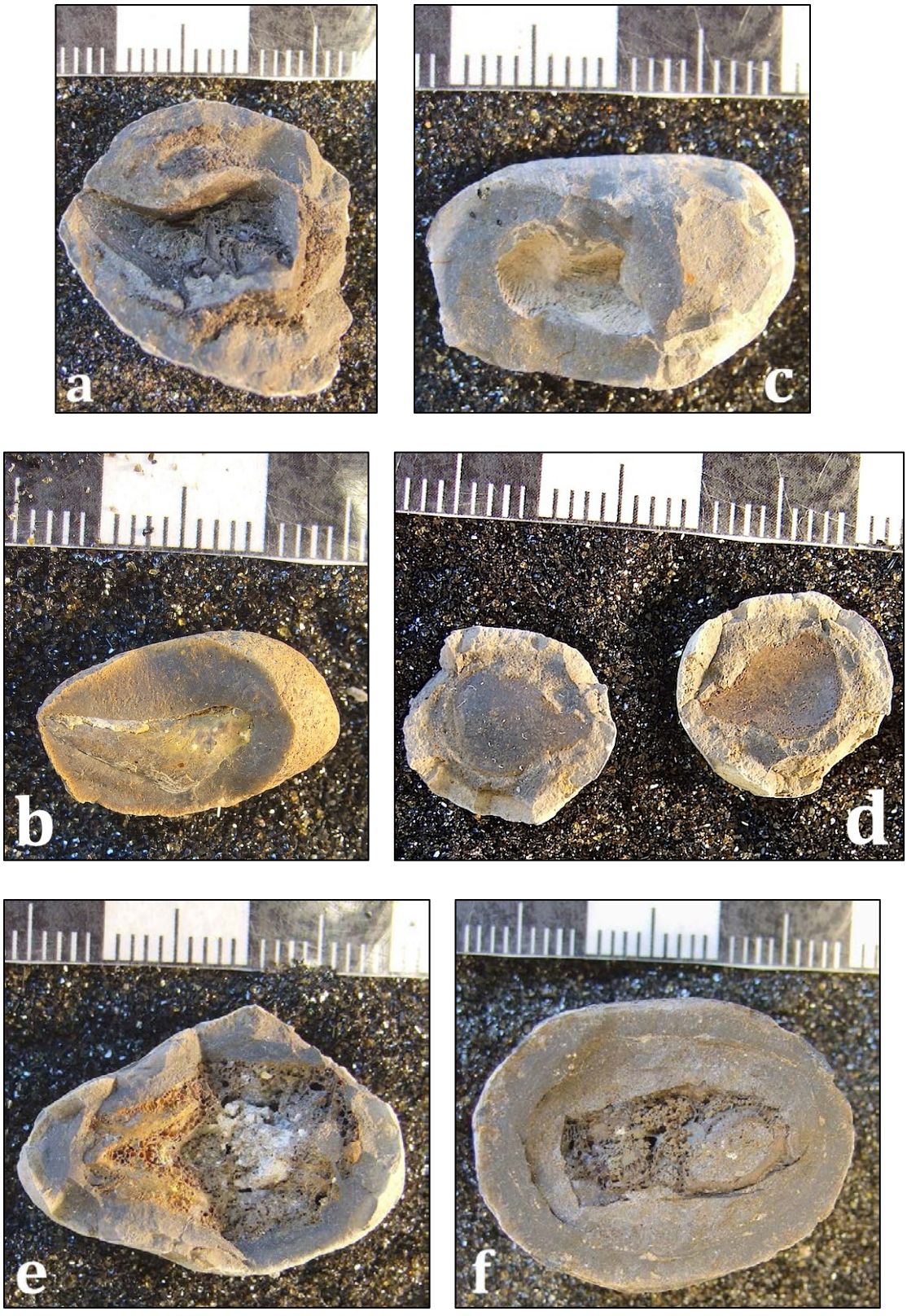

Figure 3: Nodules containing the remains of paleoniscid fishes. (a-c): Pieces of fish bone. (d): A fish scale. (e): Braincase (dorsal view). (f): Braincase (lateral view).

Chondrichthyans are represented by pieces of cartilage (Fig. 4), as well as the distinctive dermal spines that characterize the holocephalid genus *Listracanthus* (Newberry and Worthen 1870). Other chondrichthyan taxa from this time period include the Symmoriiformes and Xenacanthiformes (stem elasmobranchs), and the Iniopterygiformes, a group of stem chimaeroids (Pradel, personal comm., 2013). However, it cannot be determined which, if any, of these groups are represented by the fossilized cartilage found in the nodules.

It is also possible that some of the cartilage and/or unidentified vertebrate remains represent members of the Acanthodii, an extinct class of early jawed fishes that shared characteristics with both bony fish and chondrichthyans. Acanthodian remains have been recovered from similar phosphatic concretions from Carboniferous shales elsewhere in the Midcontinent (Dalton et al. 1998). As of yet, however, no fossils from the sample have been identified as acanthodian.

Figure 4: Nodules containing pieces of chondrichthyan cartilage. Note the characteristic prismatic structure of the fossilized cartilage.

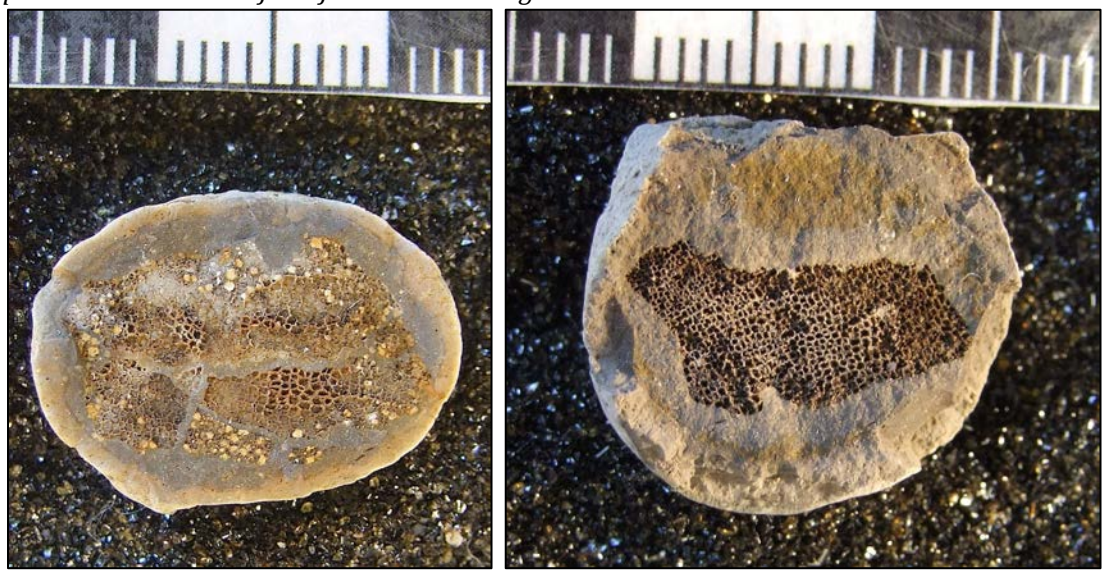

The invertebrate remains are dominated by cephalopod fossils, present primarily in the form of ammonoid shell material. Although much of the material is fragmentary, one ammonoid is sufficiently complete that it can be positively identified as *Pennoceras*, the index fossil for the horizon where the nodules were collected (Boardman et al. 1994). Pieces of nautiloid shells, although less common than the ammonoids, are also present, as well as orthoconic shells that may represent either nautiloids or coleoids. Two nodules were also found to contain coleoid arm hooks. Notably, rare cephalopod mouthparts have been found within nodules from this locality. Out of the 1,876 nodules sampled, one contained a cephalopod jaw of unknown affiliation (Fig. 5), while another contained a radula associated with ammonite shell debris.

Figure 5: Cephalopod remains. Left: Nodule containing cephalopod jaw. Right: Shell of coiled ammonoid or nautiloid protruding from nodule.

50% of the identifiable invertebrate remains can be definitively classified as cephalopods (Table 1). Another ~17 % consist of shell material that cannot be

identified beyond the phylum level; much of this material is fragmentary or extensively weathered. There is no evidence of the presence of other molluscan groups, such as bivalves or gastropods. After the cephalopods, the brachiopods are the second most commonly represented invertebrate group in the assemblage; brachiopod fossils comprise 25% of identifiable invertebrate remains. All brachiopod specimens recovered are inarticulate orbiculoids, characterized by their round shape and pronounced concentric growth lines (Fig. 6). By far the least common of the invertebrate taxa found in the nodules are arthropods, which make up the remaining ~8% of invertebrate specimens. The pieces of cuticle that constitute the sole arthropod remains (Fig. 6) cannot be identified at the subphylum level. It is possible that these fossils represent something similar to the Upper Pennsylvanian malacostracan crustaceans described by Schram (1984), which were recovered from a geologic setting very similar to that under consideration here.

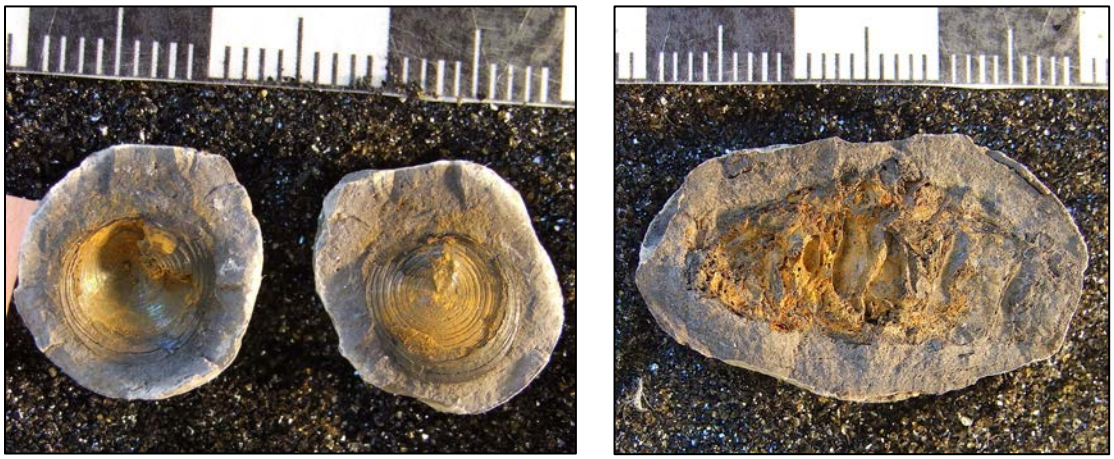

Figure 6: Nodules containing invertebrate remains. Left: An orbiculoid brachiopod. Right: Crushed arthropod cuticle.

A single nodule containing fossilized plant remains is present in the sample (Fig. 7). The plant material, found in a nodule that was unusually large and flat, consists of a

single axis with short protrusions on either side. The plant has been identified as a conifer (Mapes, personal commun., 2013). This fossil must therefore represent a very early example of the coniferous plants, which first appeared in the fossil record in the Pennsylvanian (Henry 2005). It is also the only specimen in the sample that preserves material that is clearly terrestrial in origin.

Figure 7: Nodule containing plant material identified as a conifer.

In total, approximately a third (~34.1%) of all the nodules in the sample contained identifiable fossil material. However, only ~26.2% of the nodules can be definitively classified as empty. The remaining ~39.7% of the nodules contain structures that cannot be positively identified as organic with the naked eye or simple light microscopy.

Elemental analysis via energy-dispersive X-ray spectroscopy works best when the sample being analyzed is a polished thin section or other completely smooth surface (Hafner 2013). Given the rough texture of the nodules, the quantitative data from

the EDX analyses are likely to be inaccurate. However, energy-dispersive X-ray spectroscopy is still useful for determining the elements that are present and their relative abundances. EDX analysis reveals that the fossil material in the nodules is preserved largely in calcium phosphate (see Appendix). Smaller amounts of carbon are present in the majority of the specimens examined. Some nodules contain traces of aluminum and silicon, while others are comparatively enriched in these elements, suggesting the presence of aluminosilicate minerals. Iron and potassium are also present as trace elements. Although elemental composition varies between nodules, the composition of the fossil material in a given nodule is rarely different from that of the sediment matrix.

When examined under SEM, at least two distinct types of phosphate mineralization can be observed: small, randomly oriented granules and elongated, radially oriented crystals. In several specimens, the phosphate granules that have replaced the original material are encrusted with a rind of elongated crystals growing perpendicular to the coating surface (Fig. 8). These crystals thicken centrifugally and form bundles, producing a characteristic "cauliflower" texture on the surface of encrusted material.

The contents of all eleven nodules containing crushed fossil material exhibit some degree of coating by these needle-like crystals. When examined with the naked eye or under a light microscope, the eleven nodules appear to exhibit considerable variation in the color, shape, and texture of their fragmented contents; this suggested that the nodules might differ in their fossil content or means of

preservation. SEM, however, reveals that every surface is covered in the botryoidal texture produced by phosphatic encrustation (Fig. 9). The original microstructure of the crushed material has thus been completely obscured.

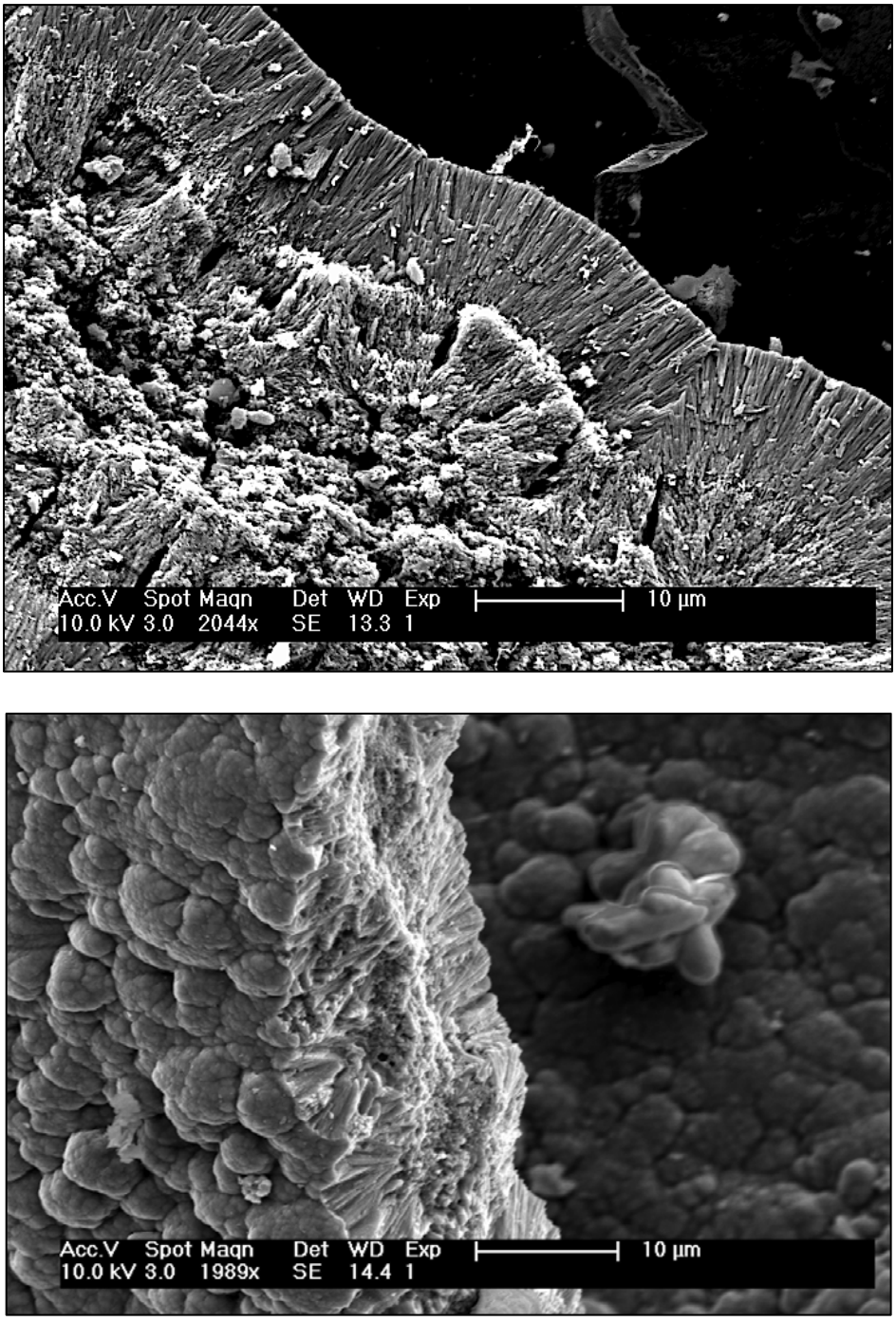

Figure 8: SEM images of encrusted fossil fragments from two nodules containing crushed material. Note the characteristic texture of phosphatic encrustation in cross-section (top) and on the surface (bottom).

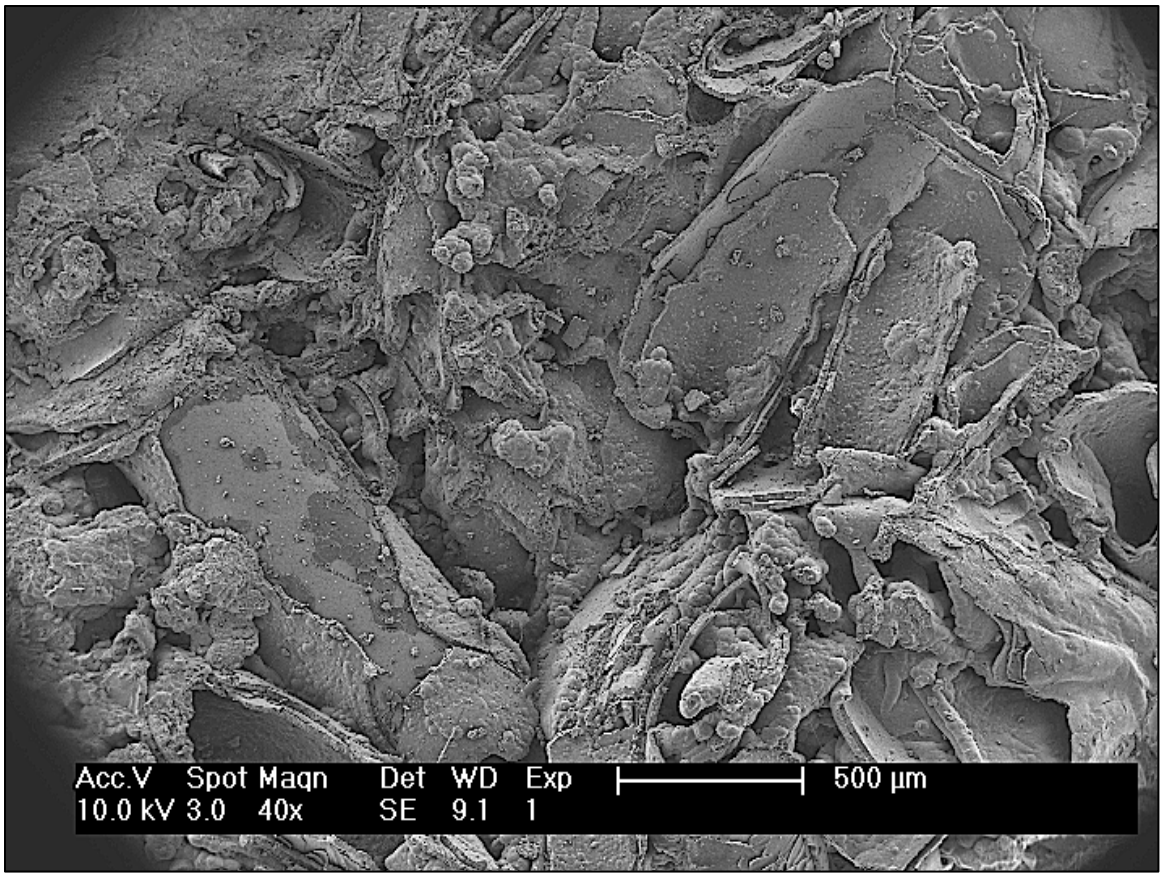

Figure 9: Overview of a portion of the crushed material inside a nodule. Note the extensive encrustation and overgrowth covering the surfaces of the fragments.

In contrast, the intact fish bones and pieces of cartilage examined under SEM do not appear to be encrusted. Notably, one fish bone exhibits encrustation only where it has been broken. This specimen has been damaged in such a way that a portion of the surface has collapsed, revealing the internal cavity of the bone (Fig. 10). The inner surface of the cavity, as well as the bone fragments therein, are entirely encrusted. Elsewhere on the bone, where the surface is unbroken, no encrustation is visible. This differential phosphatization suggests that there may be a relationship between breakage or degradation of the fossil material and the extent to which it is encrusted.

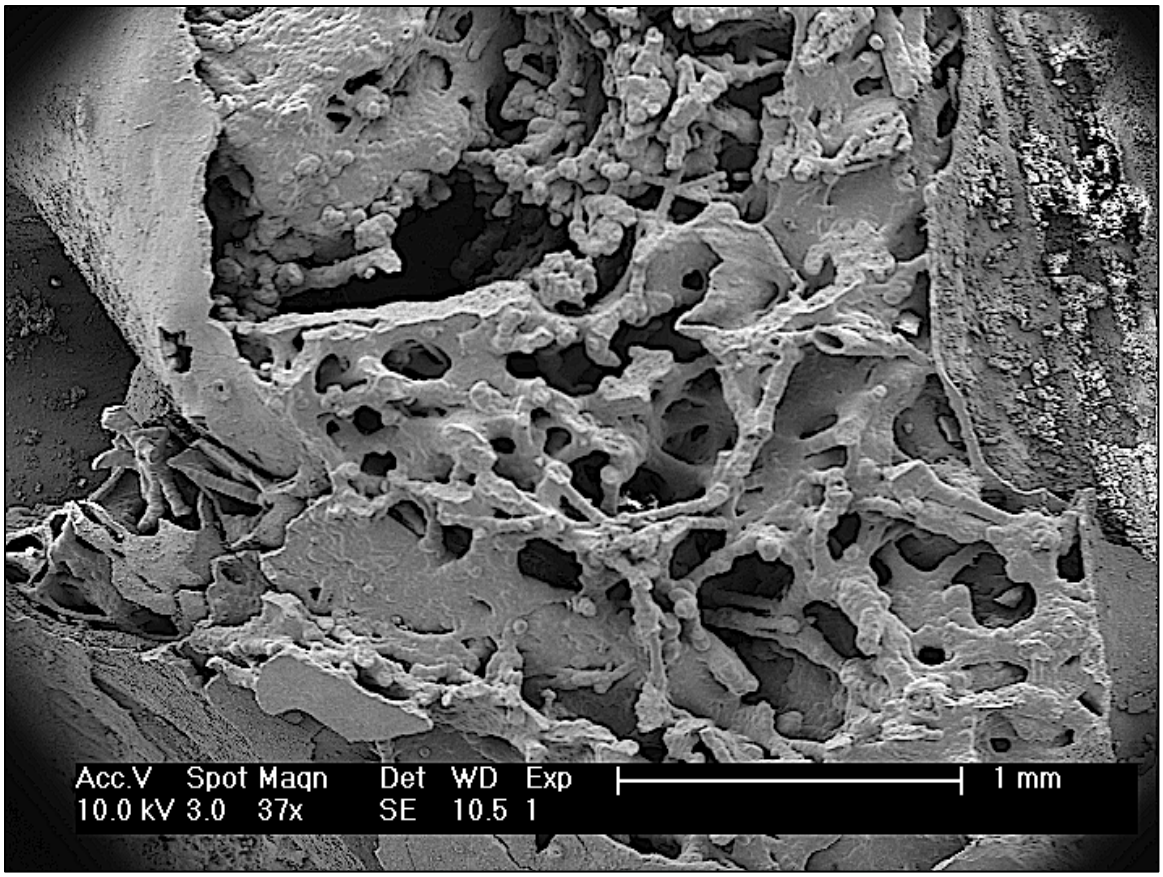

Figure 10: Overview of broken region of fish bone. Note the extensive overgrowth and presence of encrusted filaments.

Several of the nodules contain filamentous or tubular structures that are visible under the electron microscope (Fig. 10-13). In some cases, the filaments are restricted to small clusters; in other nodules they spread over a wide area. These structures run between pieces of encrusted fossil material, and in some cases form branching networks of tubes in the cavities of a larger fossil. A cross-section of one such structure reveals a central hollow tube composed of small crystal granules, surrounded by phosphate overgrowth radiating outward. Other broken filaments are visibly hollow, but lack the inner layer seen in this specimen. It is possible that in these cases the inner tube degraded after encrustation, or that the structure was recrystallized such that the inner and outer layers can no longer be differentiated by

crystal shape. Filaments that are solid in cross-section may represent instances when the original organic substrate was entirely replaced by phosphate (Yue and Bengtson 1999, p. 192).

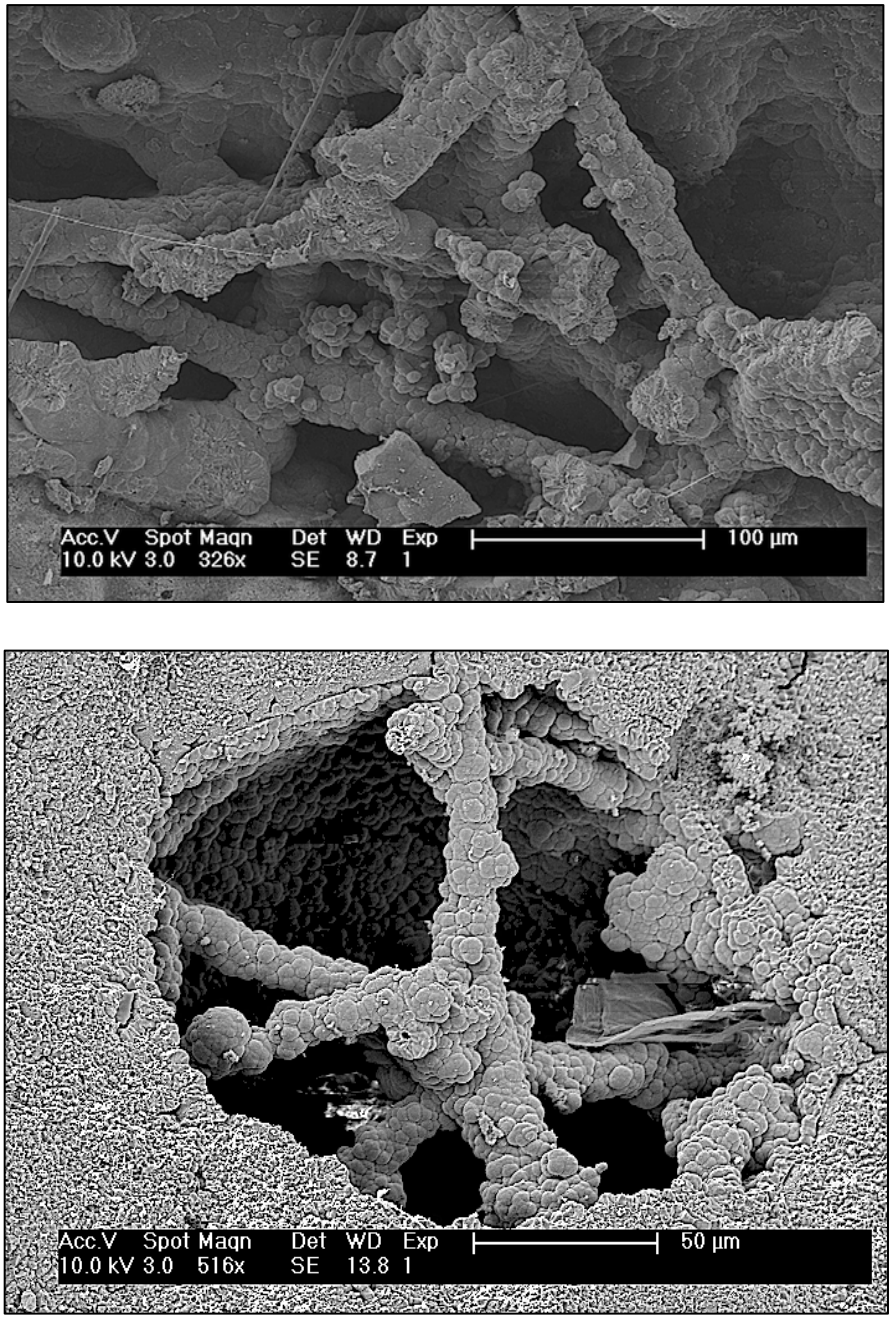

Figure 11: Encrusted filamentous or tubular microstructures. Top: A network of filaments between pieces of similarly encrusted fossil material. Bottom: A "pocket" of filaments in the sediment matrix. Note that the entire interior surface of this "pocket" has the same botryoidal texture as the filaments, which is not seen in the surrounding sediment.

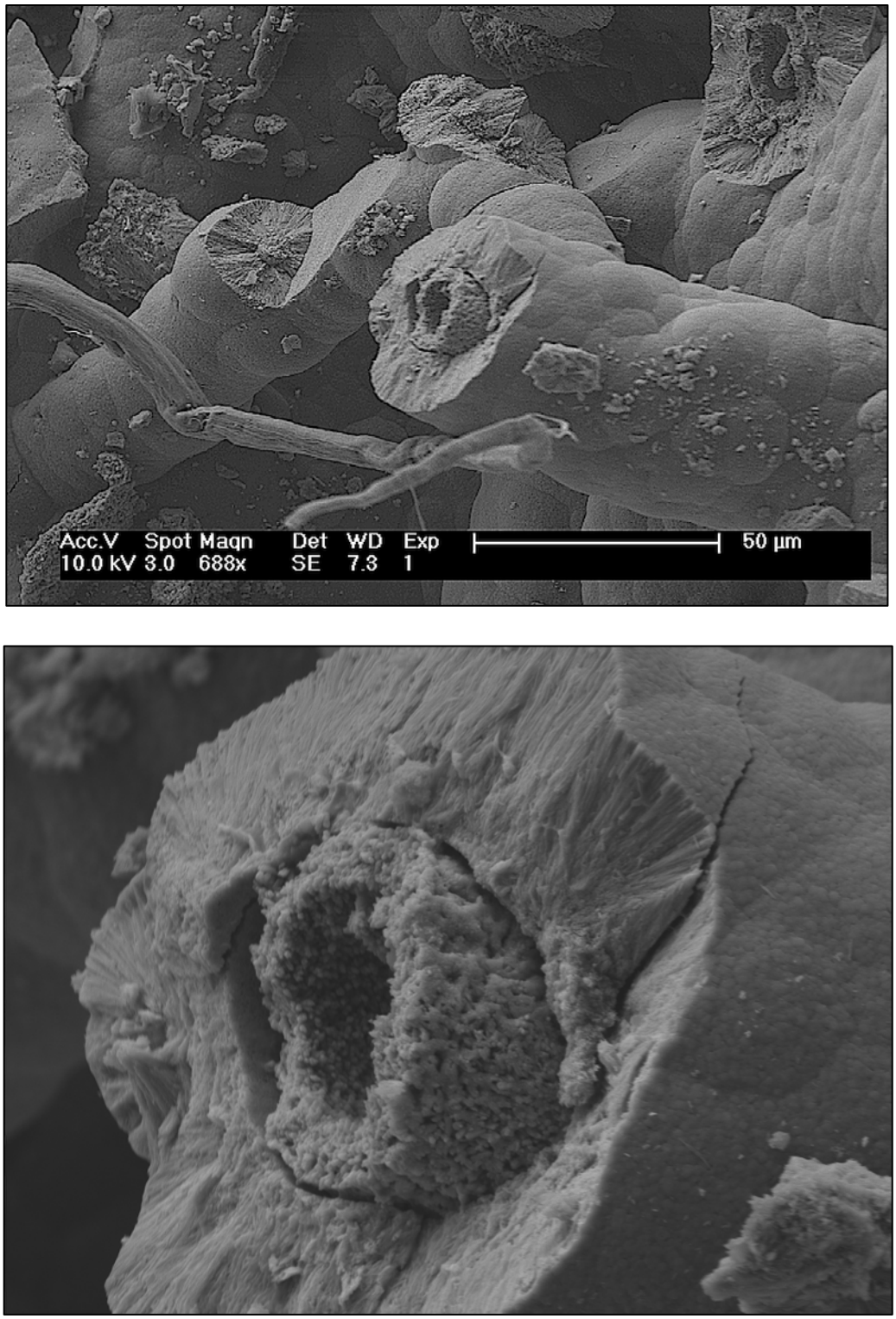

Figure 12: Overview (top) and detail (bottom) of broken tubular microstructure with hollow cross-section. Note the two distinct layers observable in cross-section, an outer rim of cauliflower-like texture encrusting an inner tube composed of small granules.

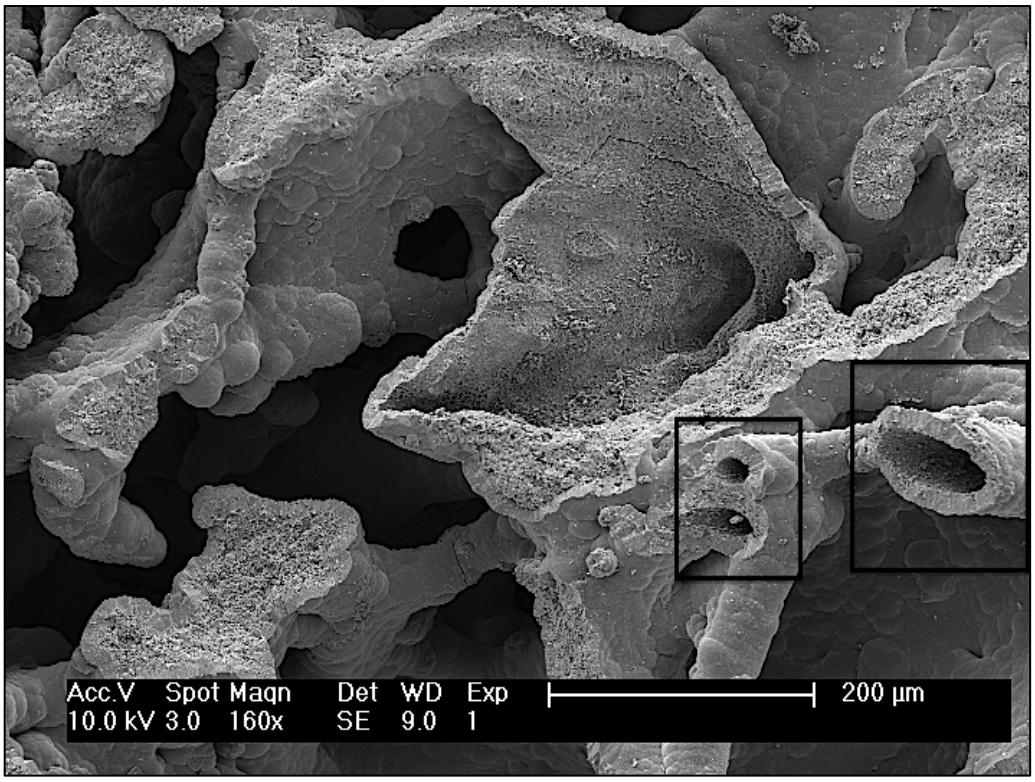

Figure 13: Detail of encrusted, broken fish bone in Fig. 10. Note that the hollow filaments (outlined in black) appear to be composed of only a single layer of crystals, lacking the inner tube seen in Fig. 12.

More rarely, portions of certain nodules reveal a strange texture under SEM. When magnified ~500x, this texture resembles a layer of hairlike or rootlike structures. Under higher magnifications (>1000x actual size), the texture appears "drippy" or "runny", like a viscous substance in the process of trickling down the surface. Granules or crystals underneath this layer appear rounded at the edges, as if coated in a layer of slime. Interestingly, this texture has developed on two different substrates. In one specimen, it overlies encrusted fossil fragments; in another, it has formed directly on top of the grains of the sediment matrix (Fig. 14 and 15).

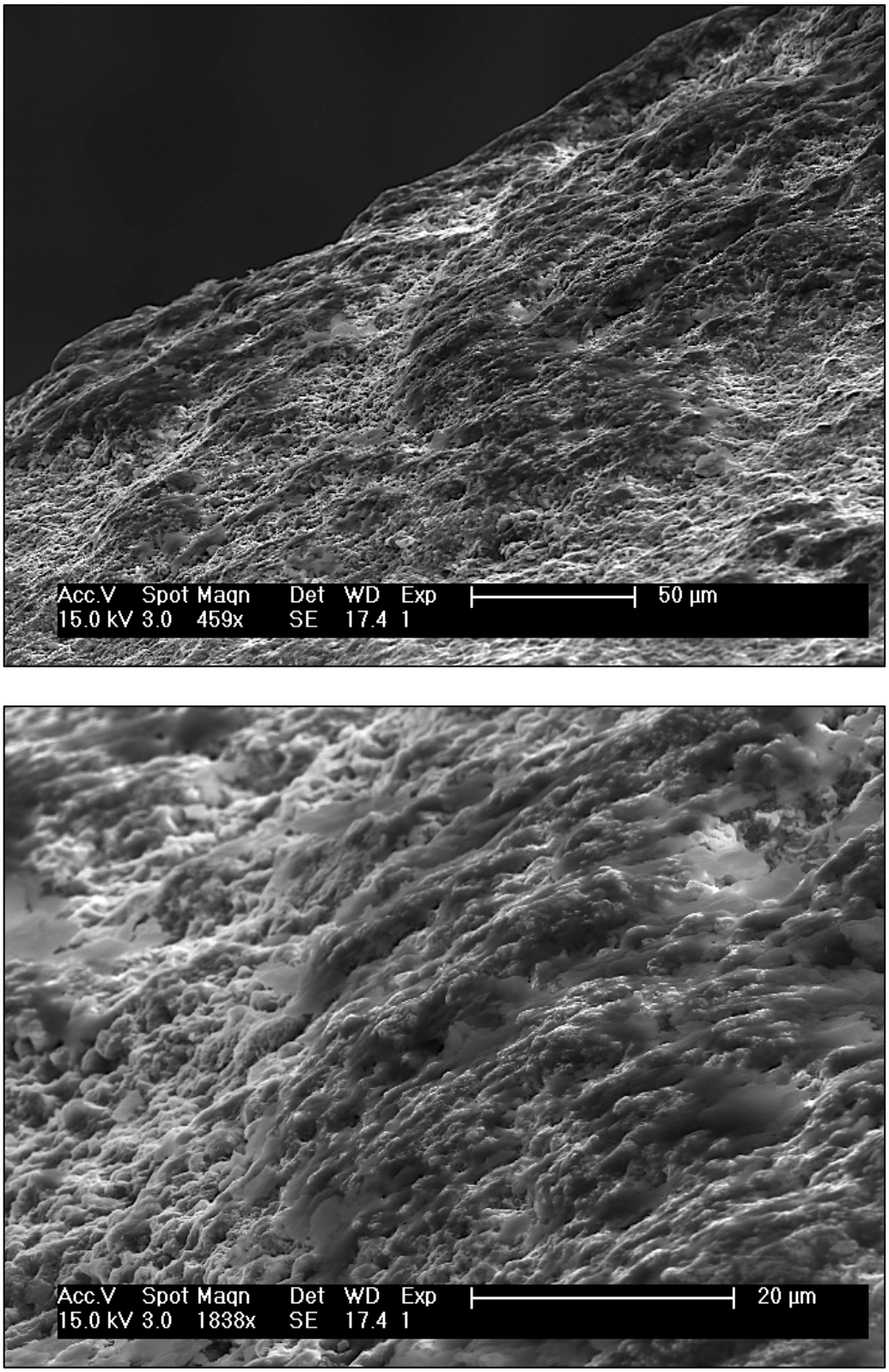

Figure 14: Overview (top) and detail (bottom) of hairlike, polymerous layer overlying sediment matrix.

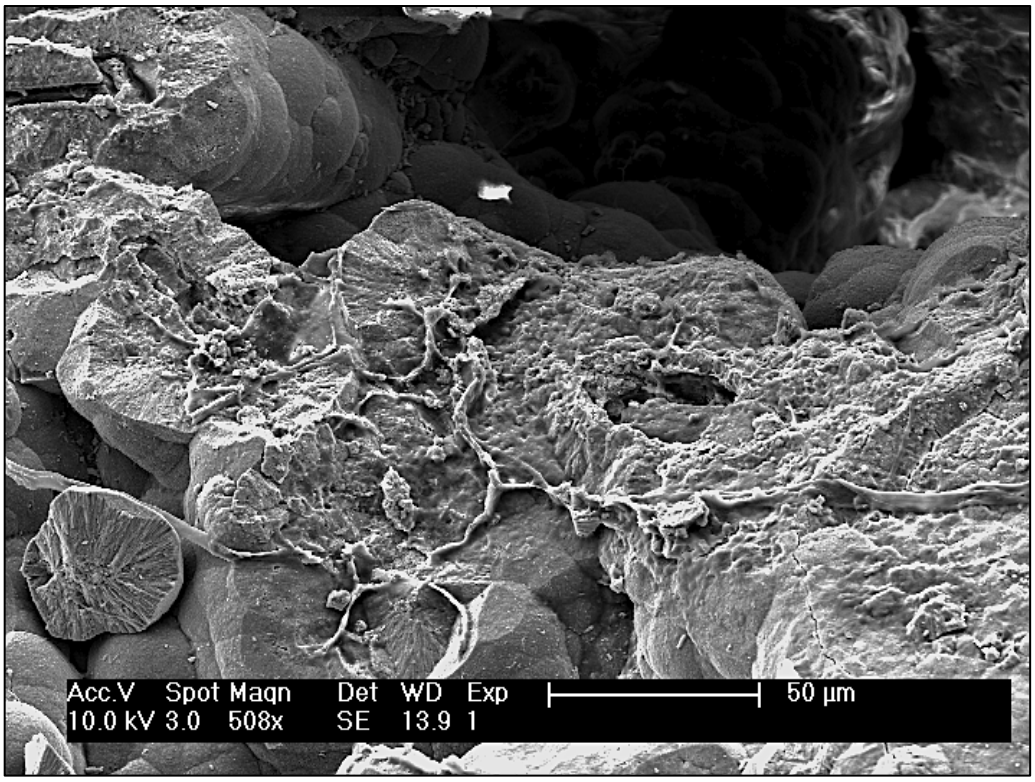

Figure 15: Hairlike texture overlying fragments of encrusted fossil material.

Discussion

Macrofossil content of nodules

One striking characteristic of the material recovered from the nodules is the extent to which the fossils are disarticulated. Rarely, if ever, are two or more adjacent body parts preserved together. For example, with the exception of the nodules containing braincases, there is never more than a single fish bone in any one nodule in the sample. Even the braincases, although technically composed of multiple bones (Wheeler and Jones 1989, p. 98), are always preserved as individual units, with no trace of any adjoining skull or jaw bones. Similarly, none of the nodules in the sample contain more than one scale or spine. Rare aggregations of *Listracanthus* spines preserved in 3D have been recovered from locality OKM-40, but none were present in this sample (Pradel, personal comm., 2013). Neither are there any

nodules that contain multiple individual organisms, e.g. more than one brachiopod. Thus, most of the nodules examined seem to have formed around isolated pieces of fossil material rather than aggregations of specimens.

However, the nodules containing pulverized material (Fig. 16) may be an exception to this generalization. For instance, they may represent coprolites or regurgitates composed of the remains of various prey animals. However, destruction of the microstructure of the fossil fragments during phosphatization makes it difficult to discern whether multiple types of organisms are represented in the crushed material from a single nodule. Furthermore, even if the microstructure were preserved, a nodule containing crushed material from multiple organisms of the same species could not readily be distinguished from the crushed remains of a single organism. Therefore, it is possible that the apparent prevalence of nodules containing individual fossils is an artifact of taphonomy, because nodules containing the remains of multiple individuals are difficult to identify as such.

Figure 16: Nodules containing crushed material.

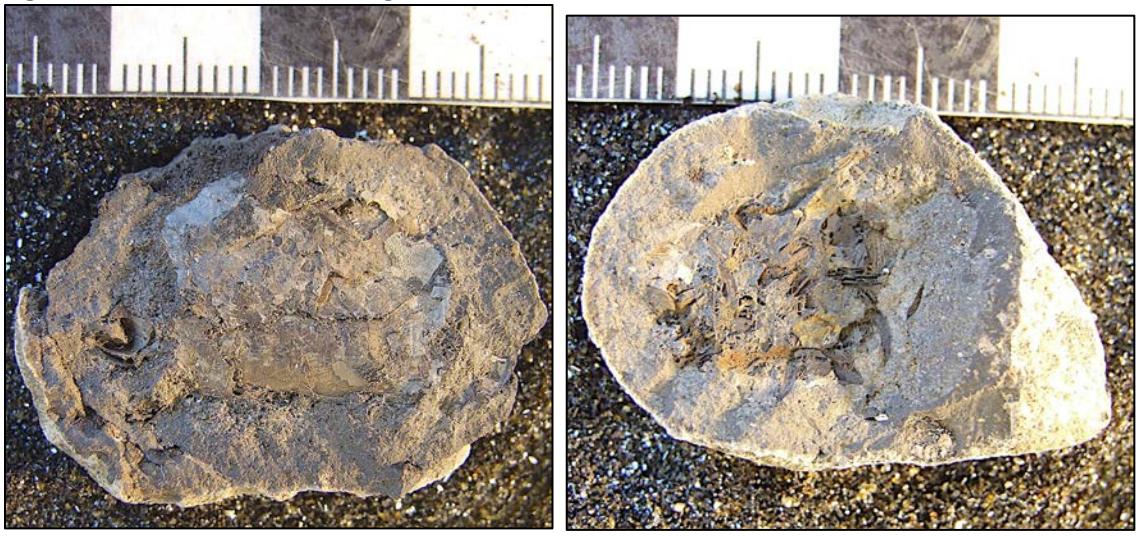

Given the anoxic, seemingly inhospitable conditions required for the deposition of the black shale and formation of the nodules, the presence of orbiculoid brachiopods in the concretions is, at first glance, unexpected. Indeed, benthic fossils are generally absent from "core" shales and the nodules therein (Heckel 1991, p. 262). However, rare benthic organisms, including brachiopods, are present in certain horizons. Concretions from the black shales of the Illinois Basin, for example, preserve gastropods, bivalves and brachiopods (Maples 1986, p. 514). Stomatopods and other benthic arthropods, preserved as organic and pyritized residues and impressions in the shale, have been collected from multiple black shales in Iowa and Nebraska (Schram 1984).

These instances reflect points at which bottom waters became more oxygenated due to relatively short-term variations in the pycnocline (Schram 1984, p. 199; Maples 1986, p. 514; Heckel 1991, p. 266; Malinky and Heckel 1998, p. 313). Such periods of increased oxygenation were too brief to be preserved as lighter-colored shale layers, but long enough to allow opportunistic aerobic organisms to establish small populations (Heckel 1991, p. 266). These organisms would be susceptible to mass death events when the bottom water returned to an anoxic state, and some assemblages of benthic fossils may represent such catastrophes (Schram 1984). Aerobic faunas that exploit temporary oxygenation of the normally anoxic seafloor were called "exaerobic" by Savrda and Bottjer (1987) and "epioxic" by Heckel (1991, p. 266).

Although a brief period of benthic oxygenation could account for the presence of the orbiculoid brachiopods in the sample, it is not the only possible explanation. In their study of the Fayetteville black shale of Arkansas, Zangerl et al. (1969) reported an extremely limited benthic fauna, consisting solely of tiny pelecypod bivalves and a smaller number of brachiopods. The authors proposed that these specimens were transported into the area from somewhere with more oxygenated bottom-water conditions (Zangerl et al. 1969, p. 117).

Malinky and Heckel (1998) reported a number of black core shales in which the only benthic organisms present are small pelecypods and inarticulate brachiopods. They presented an alternative explanation for this pattern: in these assemblages, the typically benthic organisms are so small that they could attach themselves to floating material and thus live in the water column (Malinky and Heckel 1998, p. 318). Since there are no other definitively benthic organisms in the Tacket Shale nodules, the possibility remains that these nodules represent a time during which bottom-water conditions were, in fact, completely inhospitable.

Microstructures in nodule contents

The distinctive texture produced by phosphatic encrustation that was observed under SEM in the OKM-40 material has been discussed in several studies dealing with phosphatization (see Ece 1990, their Fig. 12-13; Krajewski et al. 1994, their Fig. 10; Xiao and Knoll 1999, their Fig. 5B-D, F-H, 7A-G; Yue and Bengtson 1999, their Fig. 9A2, E; Xiao and Schiffbauer 2009, their Fig. 3B, D, F; Álvaro and Clausen 2010, their Fig. 3E, 4L). The various authors have used different terminology to

characterize the morphology of this texture; perhaps most frequently, it is described as “cauliflower”-like (e.g. Hirschler et al. 1990, p. 50; Xiao and Knoll 1999, p. 233; Yue and Bengtson 1999, p. 191; Xiao and Schiffbauer 2009, p. 99). This botryoidal texture is composed of spherulitic bundles of fibrous, radially growing (“acicular”) apatite crystals (Ece 1990; Xiao and Knoll 1999; Yue and Bengtson 1999; Xiao and Schiffbauer 2009).

The role of microbial activity in the formation of these crystals is a point of contention. Apatite precipitation is closely linked to microbial decomposition of organic material, which provides a major source of phosphate (Ece 1990; Krajewski et al. 1994). Furthermore, the spherulitic clusters have at times been interpreted as fossilized bacteria on the basis of a broad morphological resemblance (Krajewski et al. 1994). However, similar apatite spherules can also be precipitated in the absence of microbial encrustation (Nancollas 1984, p. 147; Hirschler et al. 1990, p. 52; Krajewski et al. 1994, p. 719; Xiao and Knoll 1999, p. 233). Without evidence from biomarkers or preservation of subcellular structures, it is difficult to prove that the encrusting apatite crystals represent phosphatized microbes (Xiao and Knoll 1999; Álvaro and Clausen 2010).

Encrusted filaments or tubes like those observed in the nodules have been reported in several different fossil groups; these structures have also been interpreted as putative microbial remains. Duncan and Briggs (1996) discovered filaments inside three-dimensionally preserved beetle larvae from the Tertiary of Queensland which they interpreted as fungal hyphae (see their Fig. *f*). Yue and Bengtson (1999, p. 192)

described phosphatized “thread-like or net-like structures” inside fossilized embryos and bodies of the Early Cambrian cnidarian *Olivooides* (see their Fig. 9). They suggested that the “threads” represented bacterial filaments or, alternatively, partially decayed soft tissue (Yue and Bengtson 1999, p. 192). Some of these structures are hollow while others are solid (Yue and Bengtson 1999, p. 192), an observation that also applies to the filaments observed in the OKM-40 nodules. The authors proposed that the central cavity of the hollow tubes indicates the location of original organic material that decayed away after encrustation (Yue and Bengtson 1999, p. 192). On other occasions, this organic material was completely replaced with phosphate, leaving behind a structure that was solid rather than hollow (Yue and Bengtson 1999, p. 192).

Similar filaments in shelly fossils from early Cambrian phosphorites were described by Álvaro and Clausen (2010, their Fig. 4C-E, 5A-H). The authors reported “tubular microstructures, relatively straight to slightly bent, up to 500 μm long and consistently 2-50 μm in diameter” that create branching networks (Álvaro and Clausen 2010, p. 92). The encrusted filaments “display uniformly broad (isopachous) rims” of “recrystallized fibrous fluorapatite crystals” (Álvaro and Clausen 2010, p. 94). These crystals, “ranging from 4 to 12 μm in length…occur in radiating arrangements and commonly coarsen centrifugally” (Álvaro and Clausen 2010, p. 94; see their Fig. 4I-K).

The authors interpreted the structures as microbial in origin based on comparisons with known microbial remains from both fossil and modern settings. “[T]he

strongest argument for biogenicity," they wrote, "is the tubular architecture of the filaments at a constant diameter and the coalescence of these filaments into pillars, three-dimensional networks, and mat-like structures" (Álvaro and Clausen 2010, p. 95). Álvaro and Clausen (2010) concluded that the Cambrian tubular structures most likely represent cyanobacterial filaments, fungal hyphae, or mucous strands. Further complicating the identification of these fossils is the possibility that they represent cyanobacterial-fungal consortia (Álvaro and Clausen 2010, p. 96).

Xiao and Knoll (1999) and Xiao and Schiffbauer (2009) described phosphatized microfossils from the phosphorites of the late Neoproterozoic Doushantuo Formation. These include filaments that resemble those reported by Álvaro and Clausen (2010) as well as those present in the OKM-40 material (see Xiao and Knoll 1999, their Fig. 7; Xiao and Schiffbauer 2009, their Fig. 5). The Neoproterozoic filaments, which were found growing within structures hypothesized to be metazoan embryos, are similar in size and morphology to the Cambrian filaments and form the same types of networks within the cavities of the embryos (Xiao and Knoll 1999, p. 231; Xiao and Schiffbauer 2009, p. 109). Like the filaments from the OKM-40 nodules, they appear to be made up of spherulitic clusters of radially-oriented fibrous crystals that coarsen centrifugally (Xiao and Knoll 1999, p. 231; Xiao and Schiffbauer 2009, p. 99).

As "phosphate crystallites in Doushantuo rocks are generally nucleated on organic substrates", it is likely that the filaments formed this way as well (Xiao and Knoll 1999, p. 231). Accordingly, Xiao and Schiffbauer (2009, p. 95) concluded that the

structures were formed via "encrustation through mineral nucleation and precipitation" on organic filaments. Cross-sections of the phosphatized tubes suggest that, prior to encrustation, the original organic filaments were less than 5 μm in diameter (Xiao and Knoll 1999, p. 231). Like Álvaro and Clausen (2010), Xiao and Schiffbauer (2009, p. 99) listed fungal hyphae, bacterial filaments, and mucous strands as possible substrates for phosphate nucleation and encrustation. Their interpretation of the fossil filaments as microbial in origin is supported by the fact that they are "almost identical in morphology" (Xiao and Schiffbauer 2009, p. 110) to the modern silicified microbial filaments described by Jones et al. (1997) and Renaut et al. (1998).

Thus, while the interpretation of the phosphate crystals themselves as microbial fossils is dubious, there exists significant evidence that the encrusted tubes present in the OKM-40 nodules represent microbial remains of some form. Given that cyanobacterial filament networks can bear a strong resemblance to fungal hyphae (Golubic et al. 2005) and mucous can be produced by any number of microbial organisms, the precise taxonomic affinity of the fossils remains unclear. It is worth noting that Golubic et al. (2005, p. 230) specified that "dichotomously branched and finely tapered ramifications" are typical of endolithic fungi but not of endolithic cyanobacteria; Álvaro and Clausen (2010, p. 92) used these exact words to describe the networks formed by the Cambrian filaments. However, whereas true dichotomous branches are indeed rare in cyanobacteria, "pseudo-branches" are fairly common (Rippka et al. 1979); the two types of branching cannot be easily differentiated if subcellular structures are not preserved. Therefore, the apparent

presence of branching in the filaments does not constitute strong evidence against the interpretation of these structures as cyanobacteria.

Álvaro and Clausen (2010, p. 96) wrote that cyanobacteria, as photosynthesizing organisms, generally "dominate intertidal and shallow-water" settings, whereas "fungi tend to be independent of light". Given the deep-water, offshore marine depositional environment in which the OKM-40 nodules were formed, there is conceivably a greater likelihood that the filaments represent fungi as opposed to cyanobacteria. It is also possible that the structures were produced by a different type of bacteria, perhaps one that is less dependent on light. Ultimately, in the absence of subcellular structures, it is difficult to discern whether these tubes represent bacterial filaments, fungal hyphae, mucous strands, or the remains of some other organism.

Summary

The OKM-40 nodules, collected from the Missourian Tacket Shale of Tulsa, Oklahoma, contain disarticulated fossils that are preserved in three dimensions. They represent a faunal community consisting primarily of bony and cartilaginous fishes, cephalopods (ammonoids, nautiloids, and coleoids), orbiculoid brachiopods, and rare, unidentified arthropods. Rare structures such as paleoniscid braincases and cephalopod radulae and hooks have been found within these nodules. Given the deep-water, anoxic depositional environment of black "core" shales, it is unsurprising that most of the organisms represented are nektonic. Infauna are completely absent, and the only definitively benthic fauna represented are small

orbiculoid brachiopods. If these shells were not transported into the area from shallower water, they may indicate a brief period of increased benthic oxygenation; alternatively, they may have lived on substrates floating in the water column.

The fossils are preserved largely by apatite replacement and encrustation of the original material. Due to this encrustation, as well as possible recrystallization, the original microstructure of the material has been obscured. This precludes identification of certain fossil remains that are crushed beyond the point of recognition. Scanning electron microscopy reveals a characteristic "cauliflower-like" texture of the encrusting apatite crystals, as well as the presence of encrusted tubular microstructures that are likely to be microbial in origin.

Only a small percentage of the fossiliferous nodules were examined under SEM; a more extensive analysis would undoubtedly provide a wealth of information regarding the fossils present and the means of their preservation. Other traces of microbial activity might be revealed by further study. Examination of thin sections of the nodules would also be informative. Furthermore, EDX analysis of these sections would provide quantitative data on the abundance of the elements present, shedding additional light on any differences in the mineralogy of the various fossils preserved. There is also much to be learned from the rarer and more complex fossils preserved in the nodules, such as the paleoniscid braincases and cephalopod mouthparts. In-depth individual studies of these fossils should therefore be performed. A more comprehensive examination of the crushed material will also be required in order to determine whether any taxonomic information survives.

It would also be worthwhile to compare the OKM-40 nodules to similar nodules from different localities, both in terms of petrology and fossil content. Similarly, a study of fossils preserved in the Tacket Shale (i.e. not within nodules) could expand our understanding of the faunal community represented at this horizon and the factors leading to the formation of the nodules. Such an analysis could also provide valuable taphonomic information if structures that are not found within the nodules (e.g. fish bones apart from the braincase) are present in the surrounding shale.

Acknowledgements

I would like to thank my advisor, Derek Briggs, and my second reader, Celli Hull. This thesis was also made possible by Isabelle Kruta, Alan Pradel, and Neil Landman (AMNH), who not only suggested the project but also provided enormous help and support throughout the research process. I am also grateful to Bushra Hussaini (AMNH) for the loan of key specimens to Yale, and to Susan Butts for receiving the loan on behalf of the department. Finally, I would like to thank Royal Mapes for his help in fossil identification, and Zhenting Jiang and Emma Locatelli for their assistance with the SEM and EDX equipment.

References Cited

Álvaro JJ, Clausen S. 2010. Morphology and ultrastructure of epilithic versus cryptic, microbial growth in lower Cambrian phosphorites from the Montagne Noire, France. *Geobiology* 8: 89-100.

Boardman DR, Mapes RH, Yancey TE, Malinky JM. 1984. A new model for the depth-related allogenic community succession within North American Pennsylvanian cyclothems and implications on the black shale problem. *In*: Hyne NJ, ed., *Limestones of the Mid-Continent*. Tulsa Geological Society Special Publication 2. p. 141-182.

Boardman DR, Work DM, Mapes RH, Barrick JE. 1994. Biostratigraphy of Middle and Late Pennsylvanian (Desmoinesian – Virgilian) ammonoids. *Kansas Geological Survey Bulletin* 232: 1-121.

Chin K. 2002. Analyses of coprolites produced by carnivorous vertebrates. *In*: Kowalewski M and Kelley PH, eds., *Predation in the Fossil Record*. Paleontological Society Special Paper v. 8. p. 43-49.

Coveney RM Jr., Watney WL, Maples CG. 1991. Contrasting depositional models for Pennsylvanian black shale discerned from molybdenum abundances. *Geology* 19: 147-150.

Coveney RM Jr., Watney WL, Maples CG. 1992. Contrasting depositional models for Pennsylvanian black shale discerned from molybdenum abundances, Reply. *Geology* 20: 89-90.

Dalton RB, Mapes RH, Kidder DL. 1998. Nuclei of phosphatic concretions from Carboniferous dysoxic and anoxic shales of Midcontinent North America. *Abstr. Program – Geol. Soc. Am.* 30(12): 12.

Duncan IJ, Briggs DEG. 1996. Three-dimensionally preserved insects. *Nature* 381: 30-31.

Ece OI. 1990. Geochemistry and occurrence of authigenetic phosphate nodules from the Desmoinesian cyclic Excello epeiric sea of the Midcontinent, USA. *Mar. Petrol. Geol.* 7: 298-312.

Emig CC. 1997. Ecology of the inarticulated brachiopods. *In*: Kaesler RL, ed. , *Treatise on Invertebrate Paleontology, Part H: Brachiopoda Revised,* vol. 1. Boulder, Colorado and Lawrence, Kansas: The Geological Society of America and the University of Kansas. p 473-495.

Fugitt FL, Kidder DL, Mapes RH. 1994. Well-preserved coprolite fabrics in Mississippian phosphate nodules from the Fayetteville Shale of Arkansas. *Abstr. Program – Geol. Soc. Am.* 26(1): 7.

Golubic S, Radtke G, Le Campion-Alsumard T. 2005. Endolithic fungi in marine ecosystems. *Trends Microbiol.* 13(5): 229-235.

Hafner B. 2013. Energy dispersive spectroscopy on the SEM: A primer. *University of Minnesota College of Science and Engineering Characterization Facility.* <http://www.charfac.umn.edu/instruments/eds_on_sem_primer.pdf>. Accessed 2014 Apr 26.

Heckel PH. 1977. Origin of phosphatic black shale facies in Pennsylvanian cyclothems of Midcontinent North America. *Am. Assoc. Petroleum Geologists Bull.* 61: 1045-1068.

Heckel PH. 1986. Sea-level curve for Pennsylvanian eustatic marine transgressive-regressive depositional cycles along midcontinent outcrop belt, North America. *Geology* 14: 330-334.

Heckel PH. 1991. Thin widespread Pennsylvanian black shales of Midcontinent North America: a record of a cyclic succession of widespread pycnoclines in a fluctuating epeiric sea. *Geol. Soc. London Spec. Publ.* 58: 259-273.

Heckel PH, Hatch JR. 1992. Contrasting depositional models for Pennsylvanian black shale discerned from molybdenum abundances, Comment. *Geology* 20: 88-89.

Henry RJ, ed. 2005. *Plant Diversity and Evolution: Genotypic and Phenotypic Variation in Higher Plants.* London: CABI. Web.

Hirschler A, Lucas J, Hubert J-C. 1990. Apatite genesis: A biologically induced or biologically controlled mineral formation process? *Geomicrobiol. J.* 8(1): 47-56.

Jones B, Renaut RW, Rosen MR. 1997. Biogenicity of silica precipitation around geysers and hot-spring vents, North Island, New Zealand. *J. Sediment Res.* 67(1): 88-104.

Kidder DL. 1985. Petrology and origin of phosphate nodules from the Midcontinent Pennsylvanian epicontinental sea. *J. Sediment Petrol.* 55(6): 809-816.

Kidder DL, Eddy-Dilek CA. 1994. Rare-earth element variation in phosphate nodules from Midcontinent Pennsylvanian cyclothems. *J. Sediment Res.* A64(3): 584-592.

Kidder DL, Hussein RAM, Mapes RH, Eddy-Dilek CA. 1996. Regional diagenetic variation in maximum-transgression phosphates from Midcontinent Pennsylvanian shales. *Geol. S. Am. S.* 306: 351-358.

Kidder DL, Krishnaswamy R, Mapes RH. 2003. Elemental mobility in phosphatic shales during concretion growth and implications for provenance analysis. *Chem. Geol.* 198: 335-353.

Krajewski KP, Van Cappellen P, Trichet J, Kuhn O, Lucas J, Martín-Algarra A, Prévôt L, Tewari VC, Gaspar L, Knight RI, Lamboy M. 1994. Biological processes and apatite formation in sedimentary environments. *Eclogae Geol. Helv.* 87(3): 701-745.

Krishnaswamy R, Fugitt FL, Kidder DL. 1994. Spiral phosphatic coprolites from the Pennsylvanian of southern Ohio. *Abstr. Program – Geol. Soc. Am.* 26(5): n. pag.

Malinky JM, Heckel PH. 1998. Paleoecology and taphonomy of faunal assemblages in gray "core" (offshore) shales in Midcontinent Pennsylvanian cyclothems. *Palaios* 13: 311-334.

Maples CG. 1986. Enhanced paleoecological and paleoenvironmental interpretations result from analysis of early diagenetic concretions in Pennsylvanian shales. *Palaios* 1(5): 512-516.

Molineux A, Mapes RH, Kidder DL, Mapes G. 1995. Phosphatic hardground lag deposits in Upper Carboniferous cyclothems in Texas and Oklahoma. *Abstr. Program – Geol. Soc. Am.* 27(6): A-371.

Murthy R, Kidder D, Mapes R, Hannigan R. 2004. Rare-earth element chemistry of Mississippian-age phosphate nodules in the Fayetteville Shale of Oklahoma and Arkansas. *Environmental Geosciences* 11(2): 99-111.

Nancollas GH. 1984. The nucleation and growth of phosphate minerals. *In:* Nriagu JO, Moore PB, eds., *Phosphate Minerals: Their Properties and General Modes of Occurrence.* Springer-Verlag, Berlin. p. 137-154.

Newberry, J.S. and Worthen, A.H. 1870. Part II—Palaeontology of Illi– nois—Section I—Description of fossil vertebrates. *In:* Worthen AH, ed., *Geology and Palaeontology*, vol. 6. Chicago: Authority of the Legislature of Illinois. p. 345–374.

Pradel A, Langer M, Maisey JG, Geffard-Kuriyama D, Cloetens P, Janvier P, Tafforeau P. 2009. Skull and brain of a 300-million-year-old chimaeroid fish revealed by synchrotron holotomography. *PNAS* 106(13): 5224-5228.

Renaut RW, Bones B, Tiercelin J-J. 1998. Rapid *in situ* silicification of microbes at Loburu hot springs, Lake Bogoria, Kenya Rift Valley. *Sedimentology* 45: 1083-1103.

Rippka R, Deruelles J, Waterbury JB, Herdman M, Stanier RY. 1979. Generic assignments, strain histories and properties of pure cultures of cyanobacteria. *J. Gen. Microbiol.* 111: 1-61.

Savrda CD, Bottjer DJ. 1987. The exaerobic zone, a new oxygen deficient marine biofacies. *Nature* 327: 54.

Schram FR. 1984. Upper Pennsylvanian arthropods from black shales of Iowa and Nebraska. *J. Paleontol.* 58(1): 197-209.

Suess E. 1981. Phosphate regeneration from sediments of the Peru continental margin by dissolution of fish debris. *Geochim. Cosmochim. Ac.* 45: 577-588.

Tanabe K, Mapes RH, Kidder DL. 2001. A phosphatized cephalopod mouthpart from the Upper Pennsylvanian of Oklahoma, U.S.A. *Paleontological Research* 5(4): 311-318.

Wheeler A, Jones AKG. 1989. *Fishes*. Cambridge: Cambridge University Press. 210 p. Web.

Williams ME. 1972. The origin of "spiral coprolites." *The University of Kansas Paleontological Contributions* 59: 1-19.

Xiao S, Knoll AH. 1999. Fossil preservation in the Neoproterozoic Doushantuo phosphorite Lagerstätte, South China. *Lethaia* 32: 219-240.

Xiao S, Schiffbauer JD. 2009. Microfossil phosphatization and its astrobiological implications. *In*: Seckbach J, Walsh M, eds., *From Fossils to Astrobiology: Records of Life on Earth and the Search for Extraterrestrial Biosignatures.* N.p.: Springer. p. 89-117.

Yue Z, Bengtson S. 1999. Embryonic and post-embryonic development of the Early Cambrian cnidarian *Olivooides*. *Lethaia* 32: 181-195.

Zangerl R, Richardson ES. 1963. The paleoecological history of two Pennsylvanian black shales. *Fieldiana Geology Memoir* 4. 352 p.

Zangerl R, Woodland BG, Richardson Jr. ES, Zachry Jr. DL. 1969. Early diagenetic phenomena in the Fayetteville black shale (Mississippian) of Arkansas. *Sediment. Geol.* 3:87-119.

Appendix: Selected EDX Spectra

Spectrum 1 – Surface of fish bone (specimen #66398)

File: E:\Wells\66398_analysis 1.pgt
Collected: April 09, 2014 13:11:26

Live Time:	100.99	Count Rate:	2828	Dead Time:	29.86 %
Beam Voltage:	15.00	Beam Current:	2.00	Takeoff Angle:	31.00

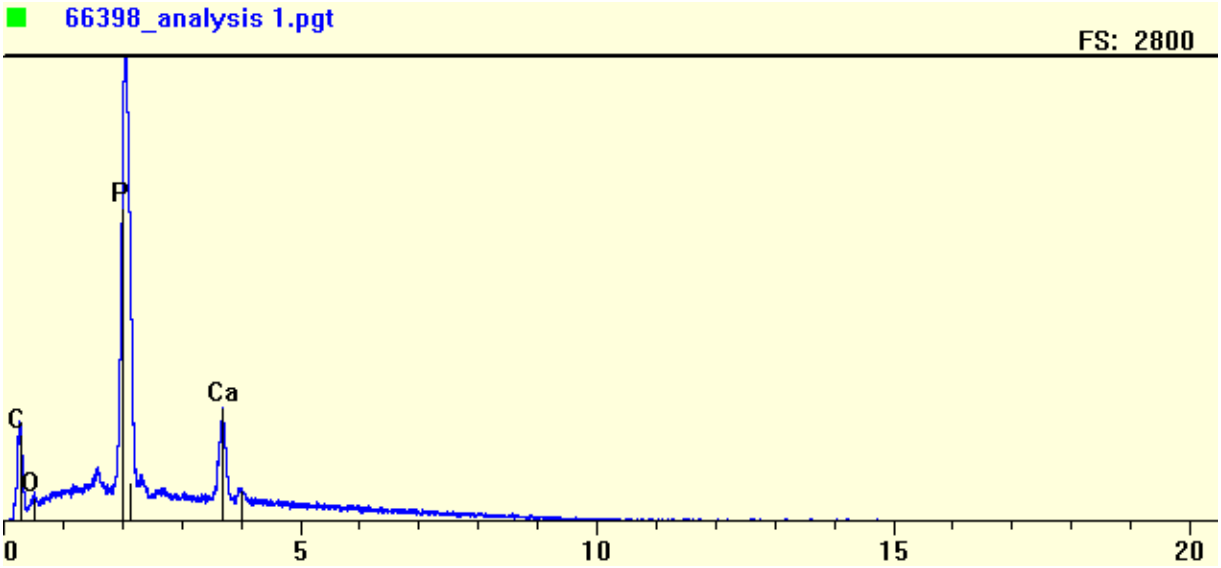

Element	Line	keV	KRatio	Wt%	At%	ChiSquared
O	KA1	0.523	0.0050	3.51	2.85	7.34
C	KA1	0.277	0.1208	85.81	92.88	7.34
Ca	KA1	3.691	0.0182	2.20	0.71	3.18
P	KA1	2.013	0.0733	8.48	3.56	557.18
Total				**100.00**	**100.00**	**203.06**

Element	Line	Gross (cps)	BKG (cps)	Overlap (cps)	Net (cps)	P:B Ratio
O	KA1	32.8	18.5	0.1	14.3	0.8
C	KA1	104.8	8.7	4.2	91.9	10.6
Ca	KA1	159.2	40.6	0.0	118.6	2.9
P	KA1	572.8	45.2	0.0	527.6	11.7

Element	Line	Det Eff	Z Corr	A Corr	F Corr	Tot Corr	Modes
O	KA1	0.038	0.976	7.139	1.000	6.963	Elmnt.
C	KA1	0.003	0.924	7.692	1.000	7.103	Elmnt.
Ca	KA1	0.797	1.146	1.053	1.000	1.206	Elmnt.
P	KA1	0.412	1.127	1.029	0.997	1.157	Elmnt.

Spectrum 2 – Sediment matrix of nodule surrounding fish bone from Spectrum 1 (specimen #66398)

File: E:\Wells\66398_analysis 3.pgt
Collected: April 09, 2014 13:45:28

Live Time:	120.41	Count Rate:	2058	Dead Time:	25.18 %
Beam Voltage:	15.00	Beam Current:	2.00	Takeoff Angle:	31.00

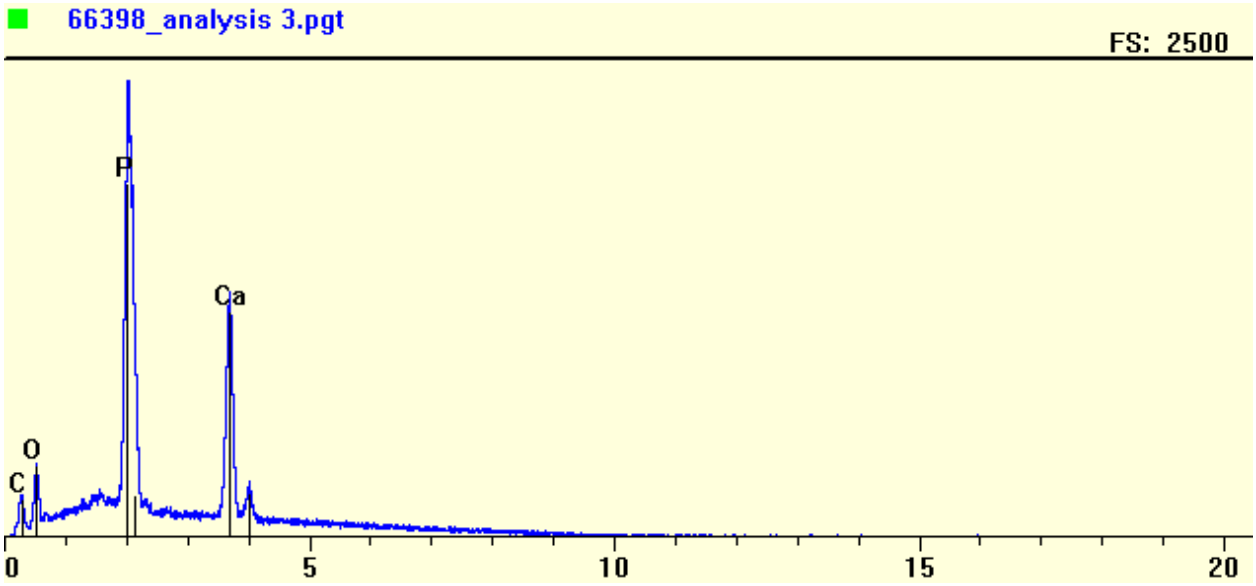

Element	Line	keV	KRatio	Wt%	At%	ChiSquared
O	KA1	0.523	0.0334	21.05	22.30	5.97
C	KA1	0.277	0.0476	42.16	59.50	5.97
Ca	KA1	3.691	0.1356	15.53	6.57	9.31
P	KA1	2.013	0.1926	21.26	11.63	243.05
Total				**100.00**	**100.00**	**85.45**

Element	Line	Gross (cps)	BKG (cps)	Overlap (cps)	Net (cps)	P:B Ratio
O	KA1	55.7	13.2	0.0	42.5	3.2
C	KA1	32.5	6.2	0.0	26.3	4.2
Ca	KA1	245.2	28.0	0.0	217.2	7.8
P	KA1	434.6	37.2	0.0	397.4	10.7

Element	Line	Det Eff	Z Corr	A Corr	F Corr	Tot Corr	Modes
O	KA1	0.336	0.895	7.049	1.000	6.305	Elmnt.
C	KA1	0.128	0.847	10.468	1.000	8.858	Elmnt.
Ca	KA1	0.910	1.052	1.089	1.000	1.145	Elmnt.
P	KA1	0.792	1.035	1.075	0.992	1.104	Elmnt.

Spectrum 3 – Surface of fish bone (specimen #66373)

File: E:\Wells\66373_01.pgt
Collected: April 04, 2014 12:27:16

Live Time:	74.63	Count Rate:	3497	Dead Time:	34.55 %
Beam Voltage:	15.00	Beam Current:	2.00	Takeoff Angle:	31.00

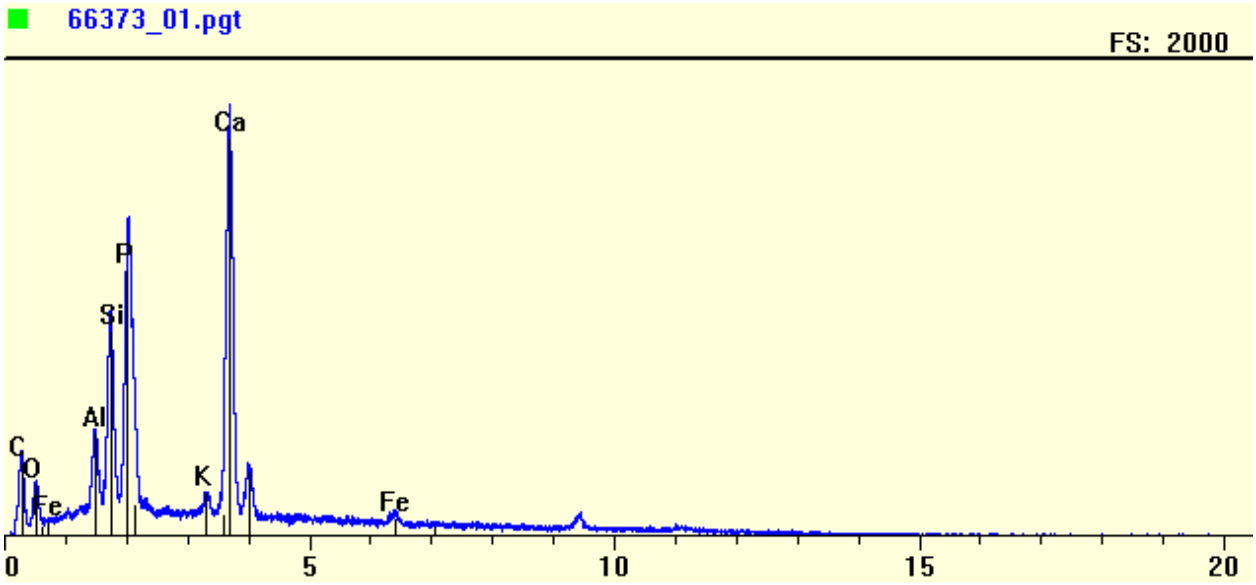

Element	Line	keV	KRatio	Wt%	At%	ChiSquared
O	KA1	0.523	0.0154	11.20	9.35	3.08
C	KA1	0.277	0.2043	77.29	85.90	3.08
Si	KA1	1.740	0.0197	2.49	1.18	69.85
Al	KA1	1.487	0.0123	1.66	0.82	69.85
Ca	KA1	3.691	0.0310	3.69	1.23	13.73
P	KA1	2.013	0.0249	3.28	1.41	69.85
K	KA1	3.313	0.0012	0.14	0.05	13.73
Fe	KA1	6.403	0.0020	0.26	0.06	1.04
Total				**100.00**	**100.00**	**28.04**

Element	Line	Gross (cps)	BKG (cps)	Overlap (cps)	Net (cps)	P:B Ratio
O	KA1	58.7	13.3	0.1	45.2	3.4
C	KA1	85.9	6.2	3.7	76.0	12.3
Si	KA1	270.6	33.6	0.1	236.8	7.0
Al	KA1	134.4	32.7	0.1	101.5	3.1
Ca	KA1	559.7	36.2	1.2	522.3	14.4
P	KA1	402.7	34.4	0.3	367.9	10.7
K	KA1	57.0	37.0	0.0	20.0	0.5
Fe	KA1	39.7	23.9	0.0	15.8	0.7

Element	Line	Det Eff	Z Corr	A Corr	F Corr	Tot Corr	Modes
O	KA1	0.053	1.000	7.258	1.000	7.260	Elmnt.
C	KA1	0.005	0.947	3.995	1.000	3.784	Elmnt.
Si	KA1	0.325	1.110	1.147	0.990	1.261	Elmnt.
Al	KA1	0.209	1.134	1.205	0.990	1.353	Elmnt.
Ca	KA1	0.813	1.174	1.013	0.999	1.189	Elmnt.
P	KA1	0.456	1.156	1.142	0.996	1.314	Elmnt.
K	KA1	0.762	1.196	1.026	0.964	1.183	Elmnt.
Fe	KA1	0.953	1.324	1.001	1.000	1.326	Elmnt.

Spectrum 4 – Sediment matrix of nodule surrounding fish bone from Spectrum 3 (specimen #66373)

File: E:\Wells\66373_analysis 5.pgt
Collected: April 09, 2014 12:52:06

Live Time:	106.29	Count Rate:	1158	Dead Time:	18.94 %
Beam Voltage:	15.00	Beam Current:	2.00	Takeoff Angle:	31.00

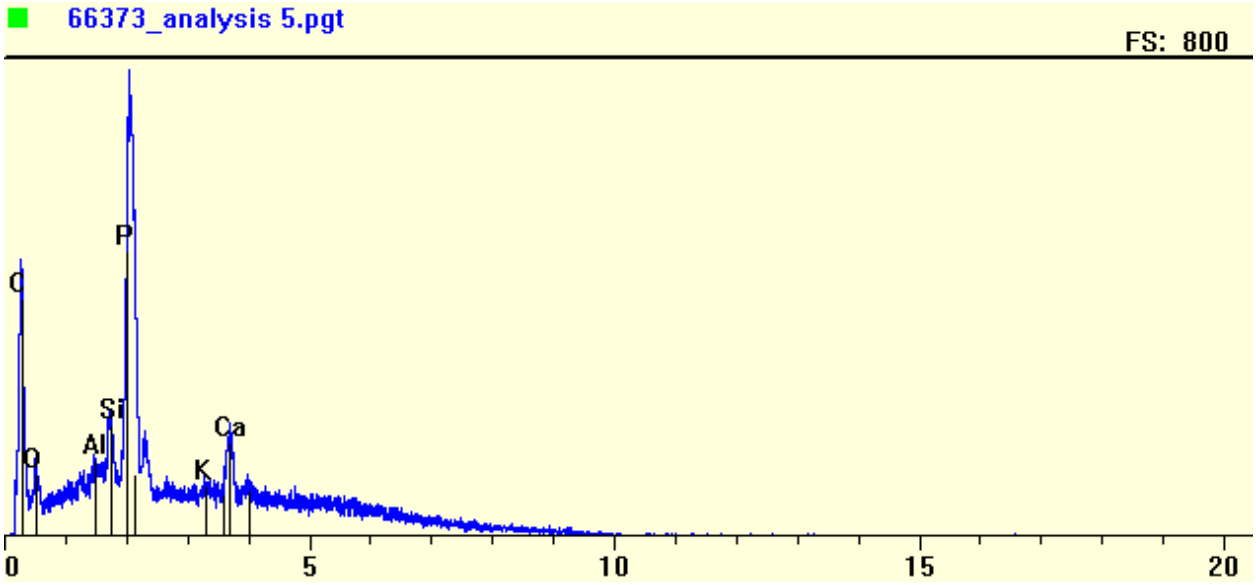

Element	Line	keV	KRatio	Wt%	At%	ChiSquared
O	KA1	0.523	0.0004	0.32	0.24	5.04
C	KA1	0.277	0.9960	99.68	99.76	5.04
Ca	KA1	3.691	0.0000	0.00	0.00	1.47
P	KA1	2.013	0.0000	0.00	0.00	96.64
Si	KA1	1.740	0.0000	0.00	0.00	96.64
K	KA1	3.313	0.0000	0.00	0.00	1.47
Al	KA1	1.487	0.0000	0.00	0.00	96.64
Total				**100.00**	**100.00**	**34.04**

Element	Line	Gross (cps)	BKG (cps)	Overlap (cps)	Net (cps)	P:B Ratio
O	KA1	22.5	9.1	0.1	13.3	1.5
C	KA1	74.6	4.3	6.5	63.8	14.9
Ca	KA1	42.4	21.6	0.1	20.8	1.0
P	KA1	141.5	24.8	0.0	116.7	4.7
Si	KA1	44.4	24.7	0.0	19.7	0.8
K	KA1	23.2	22.2	0.0	1.0	0.0
Al	KA1	30.2	23.4	0.0	6.8	0.3

Element	Line	Det Eff	Z Corr	A Corr	F Corr	Tot Corr	Modes
O	KA1	0.000	1.056	8.025	1.000	8.473	Elmnt.
C	KA1	0.000	1.000	1.001	1.000	1.001	Elmnt.
Ca	KA1	0.542	1.238	0.966	1.000	1.196	Elmnt.
P	KA1	0.062	1.218	1.015	1.000	1.236	Elmnt.
Si	KA1	0.019	1.170	1.063	1.000	1.244	Elmnt.
K	KA1	0.443	1.261	0.965	1.000	1.217	Elmnt.
Al	KA1	0.003	1.195	1.157	1.000	1.383	Elmnt.

Spectrum 5 – Piece of chondrichthyan cartilage (specimen #66401)

File: E:\Wells\66401_03.pgt
Collected: April 04, 2014 11:49:38

Live Time:	88.72	Count Rate:	4242	Dead Time:	39.14 %
Beam Voltage:	15.00	Beam Current:	2.00	Takeoff Angle:	31.00

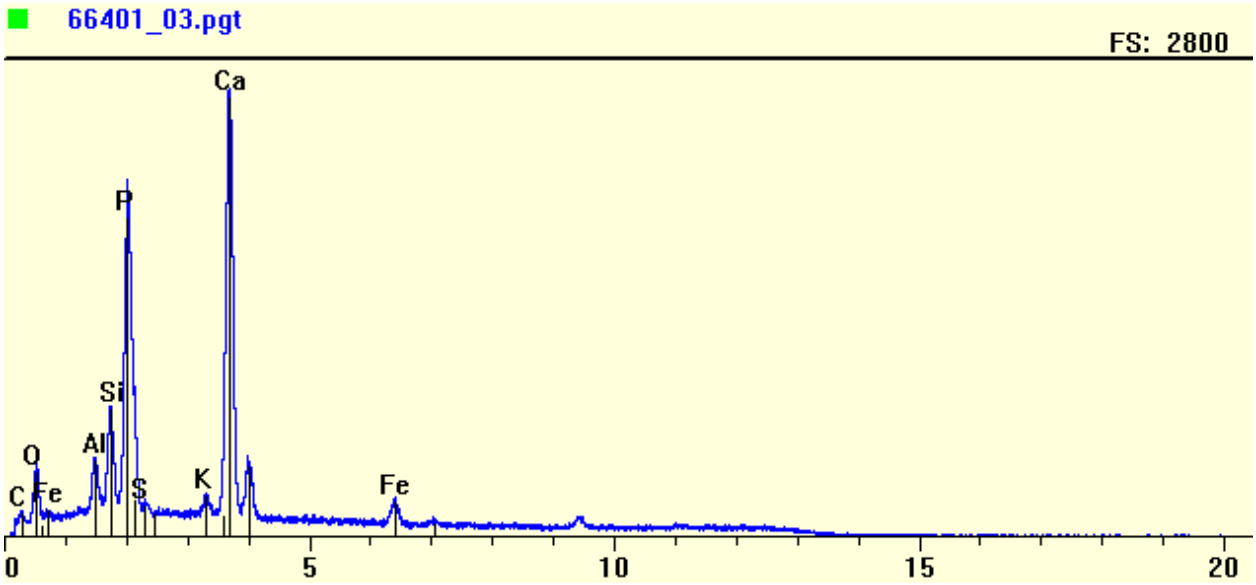

Element	Line	keV	KRatio	Wt%	At%	ChiSquared
O	KA1	0.523	0.0390	24.23	30.51	3.39
C	KA1	0.277	0.0352	23.53	39.48	3.39
Si	KA1	1.740	0.0402	4.84	3.47	65.83
Al	KA1	1.487	0.0242	3.23	2.41	65.83
Fe	KA1	6.403	0.0280	3.39	1.22	1.27
Ca	KA1	3.691	0.2167	24.02	12.08	21.11
P	KA1	2.013	0.1267	15.67	10.19	65.83
K	KA1	3.313	0.0056	0.60	0.31	21.11
S	KA1	2.307	0.0039	0.51	0.32	65.83
Total				**100.00**	**100.00**	**27.00**

Element	Line	Gross (cps)	BKG (cps)	Overlap (cps)	Net (cps)	P:B Ratio
O	KA1	89.6	17.3	0.4	71.9	4.2
C	KA1	34.7	8.1	3.9	22.6	2.8
Si	KA1	188.6	46.2	0.1	142.3	3.1
Al	KA1	121.0	44.7	0.1	76.3	1.7
Fe	KA1	69.6	31.1	0.0	38.5	1.2
Ca	KA1	705.2	44.2	1.1	660.0	14.9
P	KA1	510.7	46.7	0.2	463.9	9.9
K	KA1	63.1	45.3	0.0	17.8	0.4
S	KA1	63.0	47.4	1.3	14.3	0.3

Element	Line	Det Eff	Z Corr	A Corr	F Corr	Tot Corr	Modes
O	KA1	0.322	0.882	7.052	1.000	6.215	Elmnt.
C	KA1	0.119	0.834	8.022	1.000	6.688	Elmnt.
Si	KA1	0.703	0.980	1.256	0.978	1.203	Elmnt.
Al	KA1	0.642	1.001	1.359	0.984	1.337	Elmnt.
Fe	KA1	0.977	1.163	1.041	1.000	1.211	Elmnt.
Ca	KA1	0.908	1.036	1.072	0.998	1.108	Elmnt.
P	KA1	0.781	1.020	1.226	0.989	1.237	Elmnt.
K	KA1	0.882	1.055	1.101	0.923	1.072	Elmnt.
S	KA1	0.800	1.001	1.335	0.984	1.314	Elmnt.

Spectrum 6 – Sediment matrix of nodule surrounding cartilage from Spectrum 5 (specimen #66401)

File: E:\Wells\66401_05.pgt
Collected: April 04, 2014 12:07:32

Live Time:	78.58	Count Rate:	4848	Dead Time:	42.36 %
Beam Voltage:	15.00	Beam Current:	2.00	Takeoff Angle:	31.00

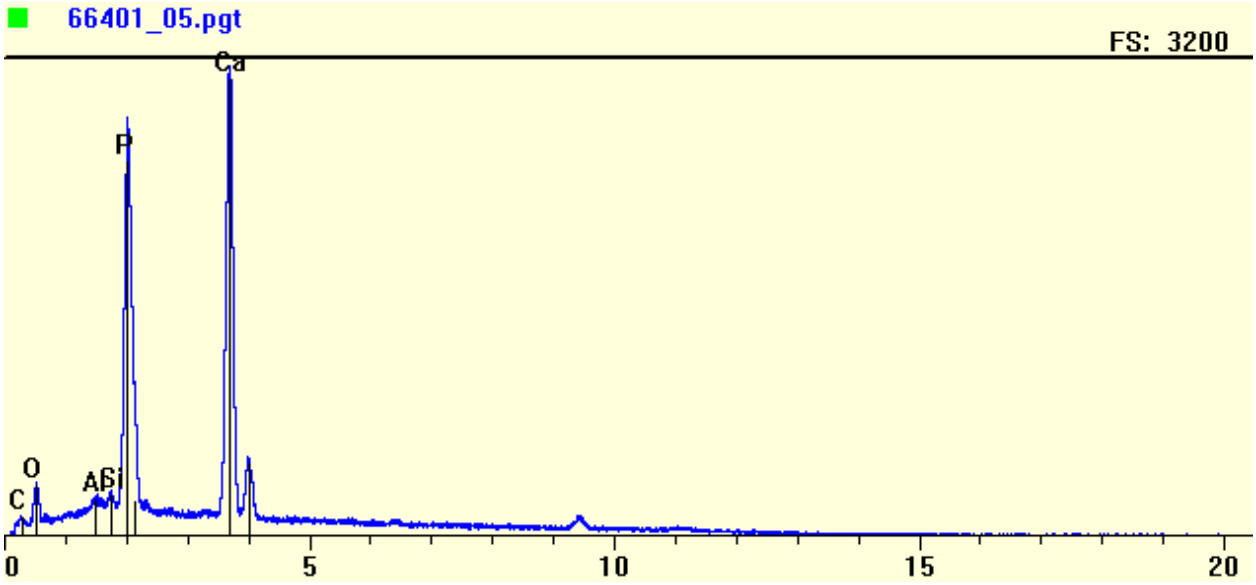

Element	Line	keV	KRatio	Wt%	At%	ChiSquared
O	KA1	0.523	0.0386	26.07	27.07	3.22
C	KA1	0.277	0.0617	41.49	57.39	3.22
Si	KA1	1.740	0.0077	0.90	0.53	114.05
Al	KA1	1.487	0.0089	1.17	0.72	114.05
Ca	KA1	3.691	0.1450	16.42	6.81	29.56
P	KA1	2.013	0.1192	13.95	7.48	114.05
Total				**100.00**	**100.00**	**43.76**

Element	Line	Gross (cps)	BKG (cps)	Overlap (cps)	Net (cps)	P:B Ratio
O	KA1	88.1	19.8	0.0	68.3	3.5
C	KA1	32.2	9.2	2.3	20.7	2.2
Si	KA1	91.9	50.3	0.1	41.5	0.8
Al	KA1	85.5	49.3	0.0	36.2	0.7
Ca	KA1	950.2	52.3	0.0	897.8	17.2
P	KA1	784.9	51.4	0.1	733.4	14.3

Element	Line	Det Eff	Z Corr	A Corr	F Corr	Tot Corr	Modes
O	KA1	0.211	0.907	7.442	1.000	6.749	Elmnt.
C	KA1	0.056	0.858	7.842	1.000	6.728	Elmnt.
Si	KA1	0.586	1.008	1.194	0.967	1.164	Elmnt.
Al	KA1	0.493	1.029	1.307	0.981	1.320	Elmnt.
Ca	KA1	0.884	1.066	1.063	1.000	1.133	Elmnt.
P	KA1	0.689	1.049	1.126	0.989	1.170	Elmnt.